UNIVERSIDAD AUTÓNOMA DE MADRID

Programa de Doctorado en Biociencias Moleculares

# Role of MYC TFs in photomorphogenesis and stomatal defense

TESIS DOCTORAL

**Andrés Ortigosa Urbieta**

Madrid, 2018

CENTRO NACIONAL DE BIOTECNOLOGIA

Universidad Autónoma de Madrid

CSIC
CONSEJO SUPERIOR DE INVESTIGACIONES CIENTÍFICAS

# UNIVERSIDAD AUTÓNOMA DE MADRID

Programa de Doctorado en Biociencias Moleculares

## Role of MYC TFs in photomorphogenesis and stomatal defense

TESIS DOCTORAL

**Andrés Ortigosa Urbieta**

DIRECTOR

**Roberto Solano Tavira**

Madrid, 2018

CENTRO NACIONAL DE BIOTECNOLOGIA

Universidad Autónoma de Madrid

# UNIVERSIDAD AUTÓNOMA DE MADRID

Programa de Doctorado en Biociencias Moleculares

Facultad de Ciencias

## Role of MYC TFs in photomorphogenesis and stomatal defense


Dr. Roberto Solano Tavira

Profesor de Investigación

DIRECTOR

Dr. Francisco Zafra Gómez

Catedrático Universidad

TUTOR

Andrés Ortigosa Urbieta

Graduado en Biología

Master en Biotecnología

DOCTORANDO


Madrid, 2018

# Table of contents

*SUMMARY* ..... 7

*ABBREVIATIONS* ..... 10

*INTRODUCTION* ..... 13

JA-Ile signaling ..... 14
Light and hormone signaling in plants ..... 15
Pseudomonas syringae and the SA/JA antagonism ..... 16
MYCs control stomata dynamics in Arabidopsis ..... 18
CRISPR/Cas9, a new technology for genetic manipulation ..... 19

*OBJECTIVES* ..... 21

*MATERIAL AND METHODS* ..... 23

Arabidopsis plant material and growth conditions ..... 24
Analysis of hypocotyl length and germination assays ..... 24
Microarray analysis ..... 24
ChIP-seq analysis ..... 25
RT-qPCR analysis in arabidopsis ..... 26
Western blot analysis ..... 26
Phylogenetic analysis ..... 26
RT-qPCR analysis in tomato ..... 27
Plasmid construction ..... 27
Tomato plant growth and transformation ..... 27
Measurements of stomatal aperture ..... 28
Pseudomonas bacterial strains ..... 28
*Pseudomonas syringae* DC3000 infection assays ..... 28
*Botrytis cinerea* infection assays ..... 28
Leaf temperature and water transpiration ratio ..... 29
Statistical analysis ..... 29
Experimental contributions ..... 29

*RESULTS* ..... 30

**Chapter 1: The JA-pathway MYC transcription factors regulate photomorphogenic responses by modulating the expression of PIF targets and HY5 ..... 31**

*myc* mutants show *phyB*-related phenotypes ..... 32
MYC photomorphogenic activity correlates with MYC levels and is partially independent of COI1 ..... 34
The COI1-independent effect of JA is dependent on interference with auxin response ..... 36
Effect of MYCs and JA in photomorphogenesis is independent on DELLAs ..... 37
MYCs are required for R-light induced gene expression ..... 40
*HY5* is a direct transcriptional target of MYCs ..... 41
MYCs and PIFs share direct targets ..... 43

**-Chapter 2: Design of a bacterial speck resistant tomato by CRISPR/Cas9-mediated editing of SlJAZ2 ... 44**

SlJAZ2 is the ortholog of AtJAZ2 ..... 45
*SLJAZ2* editing through CRISPR/Cas9 ..... 46
Gain-of-function *Sljaz2Δjas* forms prevent stomatal reopening by COR ..... 48
Dominant *Sljaz2Δjas* mutants are resistant to *P. syringe* infection ..... 49
Dominant *Sljaz2Δjas* tomato plants show unaltered levels of resistance against the necrotrophic pathogen *Botrytis cinerea* ..... 50

*DISCUSSION* ..... *51*

**The JA-pathway MYC transcription factors regulate photomorphogenic responses by modulating the expression of PIF targets and HY5** ..... **52**

**Design of a bacterial speck resistant tomato by CRISPR/Cas9-mediated editing of SlJAZ2** ..... **55**

*CONCLUSIONS* ..... *58*

*REFERENCES* ..... *61*

*SUPLEMENTARY DATA* ..... *68*

# SUMMARY

Jasmonates (JAs) are plant hormones involved in defense, development and reproduction. Activation of defences by JA is typically accompanied by the inhibition of growth. In this work, we addressed the trade-off between growth and defense through the study of MYC transcription factors (TFs), which are the main activators of JAs responses. We discovered that MYCs are required for full expression of red light regulated genes including the master regulator *HY5*. Moreover, MYC2 and MYC3 share a high number of direct targets with PIFs, and have an opposite effect on gene expression of these targets. Our results pinpoint MYCs as photomorphogenic TFs that regulate phytochrome responses by regulating PIFs targets and activating *HY5* expression. This has important implications to understand the trade-off between growth and defence, since the same TFs that activate defence responses are photomorphogenic growth regulators.

Stomata are entry ports for pathogens in plants and therefore constitute a main barrier in plant defense. *Pseudomonas syringae pv. tomato* (Pto) DC3000 is able to open stomata through the synthesis of coronatine (COR), a mimic of JA-Ile. This pathogen is the causing agent of the black speck disease in tomato. In previous works of our laboratory in the model specie *Arabidopsis thaliana*, it was discovered that MYC proteins were necessary for stomata reopening mediated by COR. In addition, this aperture could be regulated through a repressor of MYC function in the stomata, the JAZ2 protein. In this work, we confirmed the conservation of this mechanism in a crop, tomato (Solanum lycopersicum), and developed a biotechnological tool by blocking MYC function in the stomata through the CRISPR/Cas-mediated modification of *SlJAZ2* repressor. The edited version of SlJAZ2 behaves as a constitutive repressor of MYC specifically at the stomata guard cells and avoids the aperture of stomata by COR, therefore increasing resistance of tomato plants to the black speck disease caused by the pathogen Pto DC3000. Since the MYC repression by SlJAZ2 occurs specifically at stomata, MYC-dependent function in other tissues remain unaffected, such as the MYC-dependent resistance to necrotrophic pathogens.

Los jasmonatos (JAs) son hormonas vegetales con un papel en la defensa, el desarrollo y la reproducción de las plantas. La activación de defensas por JAs lleva asociada la inhibición del crecimiento. En este trabajo, estudiamos la relación entre la regulación por JAs del crecimiento y la defensa a través del estudio de los factores de transcripción (FTs) MYC. Descubrimos que los MYC son necesarios para la correcta expresión de genes regulados por luz roja, incluido el gen regulador *HY5*. Además, MYC2 y MYC3 comparten muchos genes diana con las proteínas PIFs, y tienen un efecto opuesto sobre la expresión de estos genes. Nuestros datos demuestran que los FTs MYC actúan como factores fotomorfogénicos, regulando respuestas de los fitocromos a través de la regulación de genes diana de los PIFs y activando la expresión de *HY5*. Estos datos ayudan a entender la relación entre el crecimiento y la defensa, ya que los mismos FTs que activan respuestas defensivas son también reguladores fotomorfogénicos.

Los estomas constituyen una barrera principal en la defensa vegetal ya que son puertas de entradas de bacterias. *Pseudomonas syringae pv.tomato* (Pto) DC3000 es capaz de abrir los estomas mediante la producción de coronatina (COR; mimetico de JA-Ile), lo que favorece la infección causando la enfermedad conocida como mancha negra en tomate. En trabajos previos del laboratorio en la especie modelo *Arabidopsis thaliana*, se descubrió que las proteínas MYC son necesarias para la reapertura estomática por COR. Además, esta apertura podía ser regulada de manera específica en estomas a través de un represor de la función MYC en el estoma, la proteína JAZ2. En este trabajo, identificamos el ortólogo de JAZ2, confirmamos la conservación del mecanismo en una especie de interés agronómico, el tomate (*Solanum lycopersicum*), y desarrollamos una herramienta biotecnológica para prevenir la infección mediante el bloqueo de la función MYC en el estoma a través de la edición genética del represor SlJAZ2. La versión editada de SlJAZ2 se comporta como un represor constitutivo de los MYC en el estoma y evita la apertura del estoma por COR haciendo a la planta más resistente a la mancha negra causada por el patógeno Pto DC3000. Como este efecto es específico del estoma no afecta a la función MYC en otras partes de la planta, como es por ejemplo la resistencia a patógenos necrotrofos.

# ABBREVIATIONS

| | |
|---|---|
| ABA | Abscisic acid |
| ANOVA | Analysis of variance |
| ARF | Auxin response factor |
| At | *Arabidopsis thaliana* |
| Aux/IAA | Auxin/Indole-3-Acetic Acid |
| bHLH | Basic helix loop helix |
| B | Blue light |
| Bzip | basic leucine-zipper |
| cDNA | complementary DNA |
| ChIP-Seq | Chromatin immunoprecipitation and sequencing |
| COI1 | Coronatine-insensitive 1 |
| COP1 | Constitutively Photomorphogenic 1 |
| COR | Coronatine |
| CRISPR/Cas9 | Clustered Regularly Interspaced Short Palindromic Repeats/CRISPR-associated endonuclease 9 |
| DNA | Deoxyribonucleic acid |
| DSB | Double strand break |
| ET | Ethylene |
| Flg22 | Flagellin22 peptide |
| FR | Far Red light |
| GA | Gibberellins |
| GID1 | GIBBERELLIN INSENSITIVE DWARF1 |
| gRNA | guide RNA |
| HFR1 | Long Hypocotyl in Far-Red 1 |
| HR | Homologous recombination |
| HY5 | ELONGATED HYPOCOTYL 5 |
| HYH | HY5 homologue |
| JA-Ile | Jasmonoyl-L-isoleucine |
| JA-Trp | Jasmonate-tryptophan |
| JAs | Jasmonates |
| JAZ | JASMONATE ZIM-DOMAIN proteins |
| LWL | Low white light |
| Lx | luxes |

| | |
|---|---|
| NHEJ | Non-homologous end-joining |
| NINJA | NOVEL INTERACTOR OF JAZ |
| NPA | Naphthylphthalamic acid |
| MAMPS | Microbial associated molecular patterns |
| MED25 | MEDIATOR 25 |
| MS | Murashige and Skoog |
| PACLO | Paclobutrazol |
| PCR | Polymerase chain reaction |
| PIF | PHYTOCHROME-INTERACTING-FACTOR |
| Pto DC3000 | *Pseudomonas syringae* pv. *tomato* DC3000 |
| R | Red light |
| RNA | Ribonucleic acid |
| RT-PCR | Reverse transcription PCR |
| RT-qPCR | Real time quantitative PCR |
| SA | Salicylic acid |
| $SCF^{COI1}$ | Skp1-Cul1-F-box protein Coronatine-Insensitive1 |
| SD | Standard deviation |
| SEM | Standard error of the mean |
| Sl | *Solanum lycopersicum* |
| TFs | Transcription factors |
| TIR1/AFB | Transport Inhibitor Response 1/Auxin Signaling F-Box Protein |
| TPL | TOPLESS |
| TPR | TOPLESS-related |
| WL | White light |
| WT | Wild type |

# INTRODUCTION

**JA-Ile signaling**

The phytohormone jasmonoyl-L-isoleucine (JA-Ile) and related oxilipins form a group of signalling molecules named jasmonates (JAs) that regulate many physiological processes in plants such as defense, growth and development (Wasternack and Hause, 2013).

The JA-Ile signalling cascade is well established in eudicots. In basal conditions, transcription factors (TFs) regulating JA-Ile responses are repressed by JASMONATE ZIM-DOMAIN proteins (JAZ), which recruit a co-repressor complex formed by TOPLESS (TPL) and TOPLESS-related proteins (TPR), through the NOVEL INTERACTOR OF JAZ (NINJA) adaptor (Chini et al., 2007; Thines et al., 2007; Yan et al., 2007; Pauwels et al., 2010). JAZ repressors also prevent the interaction between TFs and the MED25 subunit of the Mediator complex that links TFs to the general transcriptional machinery (Zhang et al., 2015). The JA-Ile receptor is formed by the E3-ubiquitin ligase $SCF^{COI1}$ (Skp1-Cul1-F-box protein Coronatine-Insensitive1 [COI1]), and a JAZ co-receptor (Xie et al., 1998; Katsir et al., 2008; Sheard et al., 2010). The bioactive form of the hormone ((+)-7-*iso*-JA-Ile) accumulates upon endogenous or exogenous stimuli, and is perceived by the co-receptor complex, triggering the ubiquitination of JAZ proteins and their subsequent degradation by the 26S proteasome (Fonseca et al., 2009a, 2009b; Chini et al., 2007; Thines et al., 2007). Degradation of JAZs releases the TFs, which now can activate JA responses (figure 1).

MYC proteins are a family of bHLH TFs responsible for activation of most JA mediated responses and are targets of JAZ repressors (Chini et al., 2016). MYC2 was the first family member described (Boter et al., 2004; Lorenzo et al., 2004; Chini et al., 2007). It acts additively with MYC3, MYC4 and MYC5 to regulate JA mediated processes such as root growth inhibition, fertility, and resistance to pathogens and insects (Fernández-Calvo et al., 2011; Schweizer et al., 2013; Qi et al., 2015). In addition to their role in JA signalling, MYCs have been shown to be involved in the regulation of responses mediated by ethylene, light and abscisic acid (Abe et al., 2003; Yadav et al., 2005; Song et al., 2014; Chico et al., 2014). Thus, MYCs are important hubs which integrate environmental and developmental responses (Kazan and Manners, 2013).

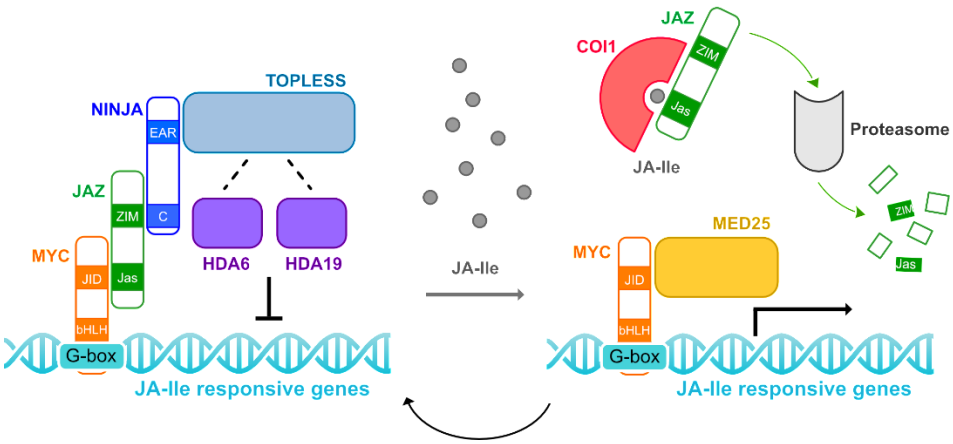


**Figure 1.** JA-Ile signaling cascade (modified from Monte, 2017). In basal conditions, MYC TFs are repressed by JAZ repressors, which recruit a co-repressor complex formed by TOPLESS through the NINJA adaptor. The JA-Ile receptor is formed by COI1 and a JAZ co-receptor. JA-Ile perception by the co-receptor complex triggers JAZ proteins ubiquitination and subsequently degradation by the 26S proteasome. Elimination of JAZs releases MYC TFs, which now can activate JA responses.

### Light and hormone signaling in plants

Plant fitness requires a continuous adaptation of plant growth to environmental conditions. Light is the most influential exogenous signal regulating plant growth and developmental plasticity (de Wit et al., 2016). It is sensed by a number of photoreceptors, including the phytochromes that detect Red (R) and Far-red (FR) light (Franklin and Quail, 2010). Phytochromes can be in two photoreversible forms, Pr and Pfr. Pr is the inactive form and after R light absorption converts into the active Pfr form, this active form reverts into the Pr form by absorption of FR. Upon R light activation, phytochromes enter the nucleus and repress PHYTOCHROME-INTERACTING-FACTORS (PIF) TFs, which are growth promoting factors in the dark (Franklin and Quail, 2010). Photomorphogenesis-promoting factors such as HY5, HYH or HFR1 are degraded in darkness by COP1. HY5 is a TF that belongs to the basic leucine zipper (bZIP) family and is a main regulator of development, controlling processes such as cell elongation and cell proliferation. HY5 inhibits hypocotyl growth and its activity is regulated by photochromes and hormone signaling cascades such as auxins or GA (Gangappa and Botto, 2016). In light, phytochromes repress COP1 activity allowing the action of positive photomorphogenic factors such as HY5, HYH or HFR1, which repress growth (for example inhibiting hypocotyl elongation in seedlings) (Deng et al., 1991; Ballesteros, 2001; Duek and Fankhauser, 2003; Lorrain et al., 2006; Leivar and Quail, 2011).

Besides light, hormones also play an important role in plant growth and developmental plasticity. Auxins are one of the main hormones in plants and are involved in plant growth and development. Auxins promote growth and its action in plants is regulated by biosynthesis, inactivation and transport. The signalling cascade is well established. Auxins are perceived by the F-box Transport Inhibitor Response 1/Auxin Signaling F-Box Protein (TIR1/AFB) auxin co-receptors, and promote the

interaction with the transcriptional repressors Auxin/Indole-3-Acetic Acid (Aux/IAA) triggering their ubiquitination and degradation. In basal conditions, Aux/IAA interact with Auxin Response Factor (ARF) TFs inhibiting auxin responses. When Aux/IAA are degraded, ARF TFs can activate auxins responses which finally lead to cell growth (Lavy and Estelle, 2016). PIF TFs are responsible of increasing auxin biosynthesis in response to shade or low light intensity therefore contributing to cell expansion. (Franklin et al., 2011; Hornitschek et al., 2012; de Wit et al., 2016).

Gibberellins (GA) are growth-promoting hormones involved in stress and developmental processes in plants, such as germination, growth and flowering. Biosynthesis of GA is also stimulated in low light or shade conditions due to the positive regulation of GA biosynthetic enzymes genes (Hisamatsu et al., 2005).

GA responses are inhibited by nuclear repressors called DELLA proteins which are repressor of PIFs (de Lucas et al., 2008; Feng et al., 2008). The signaling mechanism has been described. In basal conditions DELLA proteins accumulates in the nucleus and repress GA responses by avoiding PIFs proteins from binding to DNA. After GA biosynthesis, GA forms a complex with its receptor, GID1 and DELLA proteins. DELLA proteins are ubiquitinated and degraded, which de-repress GA responses by releasing PIFs that can now activate growth-promoting genes (de Lucas et al., 2008; Feng et al., 2008; Ballaré and Pierik, 2017).

JA influences growth by several mechanisms. For instance, JA can be conjugated with tryptophan (JA-Trp), which acts as an inhibitor of auxin transport, therefore repressing growth (Staswick, 2009; Staswick et al., 2017). JAZ repressors interact and repress DELLAs; thus JAZ degradation by JA enhances DELLA function and inhibits growth (Yang et al., 2012). Recently, JA has been shown to repress growth in darkness by MYC2-dependent inhibition of COP1 activity (Zheng et al., 2017). In our laboratory, it was found that MYC2, MYC3 and MYC4 are short-lived proteins degraded under dark or shade conditions, whereas light and JA stabilize MYC proteins in *Arabidopsis.* In contrast, JAZ repressors have an opposite regulation to MYCs since shade conditions stabilize them. This opposite regulation is the reason behind the reduction of JA sensitivity and JA-mediated defenses under shade conditions. Moreover, MYCs stability is also regulated by phytochrome B (phyB), since phyB inactivation by FR reduces MYCs stability and JA-mediated plant defenses, suggesting that destabilization of MYCs in shade could be due to phyB inactivation (Chico et al., 2014). However, the role of JA and MYCs in photomorphogenesis has not been addressed.

**Pseudomonas syringae and the SA/JA antagonism**

*Pseudomonas syringae* is a widespread bacterial pathogen that causes disease on a broad range of economically important plant species. Among them, *P. syringae* pv. *tomato* DC3000 (*Pto* DC3000) is the causative agent of the bacterial speck disease of tomato (*Solanum lycopersicum*) (Blancard,

2012). Susceptible tomato cultivars include the variety Moneymaker, which is widely used in agriculture and, therefore, economically important. Outbreaks of bacterial speck on tomatoes occur in moderate temperatures (15-25º) and wet conditions (Jones et al., 1991). Under favourable environmental conditions, disease symptoms appear as small brown necrotic spots (specks) in leaf and fruits (Bender et al., 1987). This disease affects negatively the productivity and marketability of the tomatoes (Jones et al.,1991) and causes economic losses all over the world (Schneider, 1977; Gitaitis et al., 1985).

The initial infective process of *P. syringae* relies on natural openings and accidental wounds on the plant surface to colonize internal tissues (Melotto et al., 2008). Stomata are an example of such openings, providing one of the main routes through which the foliar pathogen *P. syringae* can penetrate the leaf epidermis and start multiplying aggressively in the apoplast (Melotto et al., 2017). Stomata are pores present on the surface of the leaves that are involved in gas exchange, regulating photosynthesis and water loss through transpiration stream (Kim et al., 2010). Besides this, stomata also play an active and dynamic role in defense against pathogens being an integral part of the plant innate immunity system (Melotto et al., 2006, 2008; Zhang et al., 2008; Liu et al., 2009). Upon microbial perception, achieved by the specific recognition of conserved microbial associated molecular patterns (MAMPS) such as bacterial flagellin, via surface-localized receptors, plants rapidly close stomata (Melotto et al., 2006). This closure requires the salicylic acid (SA) and abscisic acid (ABA) plant hormones, and inhibits the entry of *P. syringae* restricting host tissue colonization (Melotto et al., 2006; Zhang et al., 2008; Zeng and He, 2010; Du et al., 2014; Gimenez-Ibanez et al., 2017). Once in the apoplast, *P. syringae* encounters apoplastic plant immunity, which also relies on a plethora of plant hormones including SA and JA. In general terms, SA defenses positively regulate resistance to biotrophic and hemi-biotrophic microbes such as *P. syringae*, whereas a combination of JA and ethylene (ET) pathways activates resistance against necrotrophic pathogens such as the fungus *Botrytis cinerea* (Robert-Seilaniantz et al., 2011). SA and JA/ET defense pathways generally antagonize each other, and consequently, elevated resistance to biotrophs is often correlated with increased susceptibility to necrotrophs, and viceversa (Glazebrook, 2005).

*P. syringae* strains such as *Pto* DC3000 have evolved a refined strategy for manipulating hormonal crosstalk by producing coronatine (COR), a mimic of the bioactive JA hormone, JA-Ile (Fonseca et al., 2009a), that binds to and activates the same COI1/JAZ co-receptor. By activating the JA pathway, COR inhibits SA-dependent defenses and thus stimulates the reopening of stomata to facilitate bacterial invasion and growth in the apoplast (Brooks et al., 2005; Laurie-Berry et al., 2006; Melotto et al., 2006, 2008; Zheng et al., 2012; Gimenez-Ibanez et al., 2017). COR acts as a potent virulence factor in plants by triggering the degradation of JAZs and activating the JA-pathway. Acquisition of COR by bacterial pathogens has been of tremendous adaptive importance during host-pathogen evolution because it has allowed bacteria to manipulate the host hormonal network to promote susceptibility.

Genetic manipulation of defense pathways has succeeded in enhancing resistance to specific kinds of pathogens. However, due to the antagonistic interactions between the SA and JA defense pathways, efforts to develop plants with broad-spectrum resistance by manipulation of hormonal signaling genes has had limited success so far because enhancement of the SA-dependent defences leads to a reduction of JA-based resistance and vice versa (Robert-Seilaniantz et al., 2011; Pieterse et al., 2012). Solving this trade-off is a major challenge in agriculture and requires uncoupling the antagonism between hormonal pathways in crops.

**MYCs control stomata dynamics in Arabidopsis**

In a previous work in the laboratory, we discovered that MYC TFs are essential for COR-mediated stomata re-aperture in Arabidopsis (Figure 2; Gimenez-Ibanez et al., 2017). Triple *myc234* mutants were impaired in stomata re-opening by COR and were very resistant to bacterial infection. In spite of the relevance of this role of MYCs in stomatal dynamics, the fact that MYC genes are not only expressed at the stomata guard cells but are also broadly expressed in other plant tissues prevented their biotechnological use since depletion of MYC function would reduce plant defences against necrotrophic pathogens. However, we also identified that a regulator of MYC TFs, the repressor protein AtJAZ2, is specifically and constitutively expressed at stomata guard cells in basal conditions and is a major COR/JA-Ile co-receptor controlling stomata dynamics during bacterial invasion in Arabidopsis. JAZ2 is hijacked by bacterially produced COR to activate the JA pathway and, thus, to suppress SA-dependent stomatal closure and promote bacterial penetration (Gimenez-Ibanez et al., 2017). This suppression of stomata closure by SA is mediated by MYC TFs. Degradation of JAZ2 by COR releases MYC TFs, which activate NAC TFs that repress SA biosynthetic enzymes and SA accumulation (Zheng et al., 2012; Gimenez-Ibanez et al., 2017). Arabidopsis *jaz2* loss-of-function mutants are partially impaired in pathogen-induced stomatal closing and are more susceptible to *Pseudomonas*. In contrast, truncated JAZ2 forms lacking the C-terminal Jas domain (JAZ2Δjas) act as gain-of-function mutations that constitutively repress MYC function and prevent stomatal reopening by COR, thus promoting resistance to bacterial penetration. The C-terminal Jas domain is responsible for the interaction with COI1 in the presence of hormone and thus, JAZ forms lacking this conserved domain are resistant to COR-induced degradation and become constitutive repressors of MYC function, overcoming the action of the phytotoxin during the entry process of *P. syringae* (Gimenez-Ibanez et al., 2017). The fact that JAZ2 function is mostly restricted to the stomata, whereas MYC TFs are expressed in the whole plant (Fernández-Calvo et al., 2011), makes that alterations in this gene do not affect the MYC function and the SA-JA crosstalk in other tissues and, therefore, *jaz2Δjas* mutants still retain unaltered resistance against necrotrophs. Our work suggested that gain-of-function mutations in JAZ2 could be used as a general strategy to block MYC function only at stomata to spatially uncouple SA-JA hormonal antagonism and to block the entry of *P. syringae* strains that

produce COR without compromising resistance to necrotrophs, which is mostly apoplastic, thus generating broad-spectrum resistance.

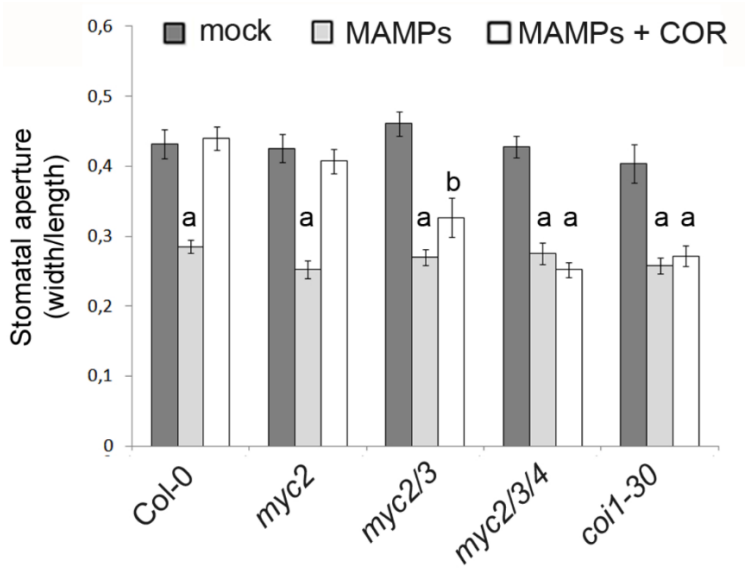


**Figure 2.** MYC2, MYC3 and MYC4 regulate COR-induced stomatal reopening in a redundant manner. Stomatal aperture in Arabidopsis Col-0, *myc2*, *myc2myc3*, *myc2myc3myc4* and *coi1-30* leaves measured after incubation with a mock control, MAMPs (*Pto* DC3000 extracts) and MAMPs plus COR or a mock control.

**CRISPR/Cas9, a new technology for genetic manipulation**

Precise edition of plant genomes by CRISPR/Cas9 is an extraordinary tool to improve crop performance. Genome edition is based in the error during DNA reparation after DNA double-strand break (DSB). Double-strand breaks can be repaired by non-homologous end-joining (NHEJ) or homology-directed repair (HDR). This last mechanism, HDR, is not error prone since it uses the sister cromatide as a template for DNA reparation. More interesting, NHEJ process is error prone, which results in disruptive insertions or deletions at targeted loci that can result in translational shifts, amino acid replacements or deletions (Mahfouz et al., 2014; Belhaj et al., 2015).

The activation of these DNA repair mechanisms is trigger by nucleases, which break DNA. For genome editing, the most promising system is know as CRISPR/Cas9 (Clustered Regularly Interspaced Short Palindromic Repeats/CRISPR-associated endonuclease 9) (Mojica et al., 2000), whose components are a bacterial DNA endonuclease and a guide RNA (gRNA). The gRNA contains a variable sequence (guide) complementary to the DNA target of interest at the 5´ end, and a sequence that is recognized by the endonuclease Cas9 at the 3´ (gRNA backbone). Recognition of the DNA target by Cas9 requires a short sequence, NGG, adjacent to the 3´end of the guide

sequence. This short sequence is called “protospace adjacent motif” (PAM) (Doudna and Charpentier, 2014; Mahfouz et al., 2014; Belhaj et al., 2015) (Figure 3).

Specificity and off-targeting are the main challenges for genome editing technologies, especially for the treatment of human diseases. In the case of plants, off-target mutations can be removed by back-crossing (Mahfouz et al., 2014). The region proximal to the PAM sequence determine the specificity between the gRNA and its DNA target, a complementary match of around 10 bases beside the PAM sequence is very important for successful cleavage by Cas9. In the distal region to the PAM sequence mismatches are permitted (Belhaj et al., 2015).

CRISPR/Cas9 has been applied in different plants and crops such as Arabidopsis, *Nicotiana tabacum*, maize or wheat. The mutation produced by CRISPR/Cas9 can generate heterozygous, homozygous or chimeric plants, depending when the mutation is originated (before the division of the first embryonic cell, later in development or independently in different parts of the plant). For example, an homozygous plant would be obtained if both alleles are repaired with the same mutation before the first embryogenic cell divides (Belhaj et al., 2015).

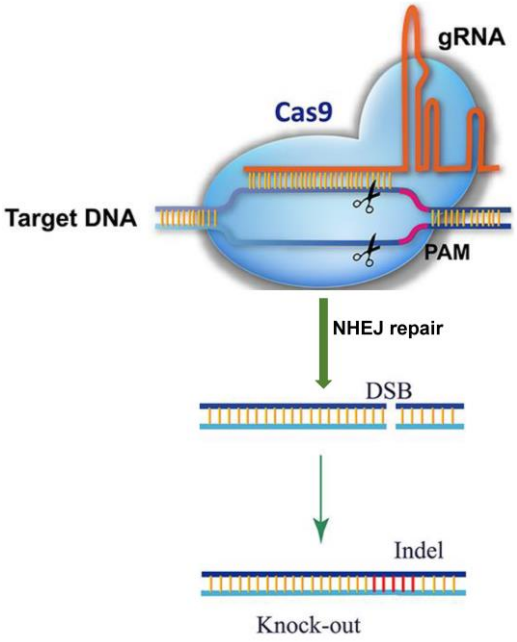


**Figure 3**. Representation of CRISPR/Cas9 genome editing (modified from Ding et al., 2016). gRNA binds to its complementary DNA, the PAM motif is necessary for Cas9 function. Cas9 breaks both DNA strands triggering double strand break repair. During the repair process, the error-prone NHEJ mechanism can introduce insertions or deletions (Indels), which can alter gene function.

# OBJECTIVES

Activation of JA-Ile signalling is associated with growth inhibition, which reduces crop yield. However, the mechanism underlying this trade-off is unknown. The fact that MYC protein stability is regulated by light and by the phytochromes suggested that MYCs could have a role in phytochrome signalling.

The **first objective** of this thesis was to understand the mechanism by which JA signaling inhibits growth by studying the role of MYC transcription factors in photomorphogenesis.

The antagonism between JA and SA pathways generate a defence trade off that difficult the generation of broad-spectrum resistance by manipulation of JA or SA pathway genes. The **second objective** of this thesis was to generate broad-spectrum resistance by manipulating the JA pathway in specific tissues. We used previous information of the role of MYC TFs and its specific JAZ2 repressor in stomata guard cells in Arabidopsis to generate CRISPR/Cas9-edited *SlJAZ2* tomato plants resistant to bacterial pathogens without negatively affecting resistance against necrotrophic pathogens.

# MATERIAL AND METHODS

**Arabidopsis plant material and growth conditions**

Arabidopsis thaliana Col-0 is the genetic background of wild type, mutants and transgenic lines used in this study. Seeds were sterilize with chlorine vapor during 2-3 hours in a crystal container. After sterilization, seeds were stratified at 4°C during 3 days in darkness. Seedlings were grown in 0.5X Murashige and Skoog (MS) medium with 1% sucrose and 0.7% agar at 21°C during 7 days (unless other time is specified) under a 16-h-light/8-h-dark cycle in a growth chamber.

For white light (WL) conditions, light intensity was 4000 lx. For low white light (LWL) conditions, petri dishes containing seedlings were covered by a filter paper (Filter lab, catalog number: 1305) and light intensity was measured as 650 lx. For specific wavelength treatments, seedlings were grown in a Percival chamber of monochromatic lights at 21°C during 6 or 7 days and exposed to continuous monochromatic Red (32$\mu$mol $m^{-2}$ $s^{-1}$), Far red (58$\mu$mol $m^{-2}$ $s^{-1}$) or Blue light (19$\mu$mol $m^{-2}$ $s^{-1}$).

Mutant lines used had been previously described as follows: *myc2 (jin1-2)* (Lorenzo et al., 2004); *myc3 (GK 445B11)*, *myc4 (GK 491E10)*, *myc2,3, myc2,4*, *myc3,4* and *myc2,3,4a* (Fernández-Calvo et al., 2011); *myc2,3,4b* and *myc2,3,4,5* (Qi et al., 2015); *jazQ* (Campos et al., 2016); *tir1afb2afb3* (Dharmasiri et al., 2005). Quintuple *della* (Feng et al., 2008). Overexpression lines 35S:MYC2, 35:MYC2-GFP and 35:MYC2-GFP,*phyB* were previously described by (Lorenzo et al., 2004; Chico et al., 2014).

**Analysis of hypocotyl length and germination assays**

For hypocotyl measurements seven days-old plants were stretched on agar plates, photographed and pictures analyzed using ImageJ software (http://www.imagej.net).

For germination experiments, plants were exposed to white light during 90 minutes after stratification, and plates were wrapped with aluminum foil and kept in dark during 3 days. Germination was accounted as emergence of the radicle from the seed after these 3 days. At least 30 seeds were evaluated per genotype. Similar results were obtained with three independent biological replicates.

**Microarray analysis**

Total RNAs from different 20-day-old plant genotypes and treatments (three biological replicates in soil) were extracted using Trizol reagent (Invitrogen), further purified using the RNAeasy Clean-Up protocol (Qiagen, Valencia, CA) and assessed quality in a Bionalyzer 2100 (Agilent), according to the manufacturers' instructions. Five hundred nanograms were amplified and Cyanine 3- (Cy3-) and Cy5-labeled using Two-Color Low Input Quick Amp Labeling Kit (Agilent Technologies). Labelled cRNAs were purified with RNeasy columns (Qiagen) and RNA yield and Cy3/Cy5 incorporation measured in a Nanodrop spectrophotometer (Nanodrop Technologies).

Preparation of probes, hybridization on Arabidopsis Oligo Microarrays 4x44K (021169, Agilent Technologies) and washes were performed as described for Agilent's 4x44k microarrays (Two-Color Microarray-Based Gene Expression Analysis, Agilent Technologies). Images for Cy3 and Cy5 channels were captured in an Agilent DNA Microarray Scanner at a resolution of 2 um, and spots quantified using Agilent Feature Extraction Software. Background correction and normalization of expression data were performed using LIMMA using the 'normexp' and 'loess' methods, respectively (Ritchie et al., 2007). Differentially expressed genes were evaluated by the non-parametric algorithm 'Rank Products' (Hong et al., 2006)and the expected false discovery rate was controlled to be less than 5%.

We considered as differentially expressed those genes with LogRatio greater than 1 or lower than -1 and the expected false discovery rate (FDR) less than 5%. We obtained a table of gene expression values across all the experiments, and simplified it by selecting just one probe per gene showing the lowest FDR value. Clustering of genes was performed using K-Means with euclidean distance (Soukas et al., 2000) in Multi Experiment Viewer (http://mev.tm4.org/).

**ChIP-seq analysis**

Chromatin immunoprecipition of MYC2 and MYC3 was performed as described (O'Malley et al., 2016), using transgenic *A. thaliana* expressing MYC2::YpET and MYC3::YpET fusion proteins from their native promoters (Gimenez-Ibanez et al., 2017). Three-day old etiolated seedlings were treated with methyl JA for 2 h (as described in(Schweizer et al., 2013)), then harvested for ChIP-Seq. Sequencing data (Zander, Lewsey, Ecker and colleagues, *unpublished*). Data were analysed as described (O'Malley et al., 2016). Briefly, reads were mapped using Bowtie2 (Langmead and Salzberg, 2012). Peaks corresponding to MYC binding sites were then identified using MACS2 (macs2 callpeak --gsize=1.19e8 -p 1e-25 --nomodel –shiftsize --down-sample --call-summits), specifying the strand shift size from cross correlation plots generated using phantompeakqualtools (default parameters) (Kharchenko et al., 2008; Zhang et al., 2008b; Landt et al., 2012; Feng et al., 2012). Within samples, identified summits were expanded to 150 nt and those with more than 10% overlap merged. High-confidence binding sites were considered to be those found in at least two biological replicates. MYC target genes were defined as having high-confidence binding-sites within 500 nt of their transcriptional start site or being the nearest gene to a high-confidence binding site, using ChIPpeakAnno (Zhu et al., 2010).

Data corresponding to chromatin immunoprecipition of PIFs were obtained from the literature (Hornitschek et al., 2012; Zhang et al., 2013; Pfeiffer et al., 2014). The lists of PIF target genes and bound PIF-sites were defined in (Pfeiffer et al., 2014). For graphical representation of PIF-bound sites, raw FASTQ data for PIF1, PIF3, PIF4 (three replicates each) and PIF5 (one replicate) were obtained

from Gene Expression Omnibus database, aligned to the TAIR10 reference genome with Bowtie2 (Langmead and Salzberg, 2012) using default parameters and BAM files converted to coverage BigWig format where replicate samples were averaged. All these steps were performed in the Galaxy platform (https://usegalaxy.org/).

Mapping of PIF binding sequences G-box (CACGTG) and PBE (CATGTG) in the TAIR10 genome sequence was performed using the 'dna-pattern' tool in RSAT (Medina-Rivera et al., 2015). Finally, BigWig files, BED files for PIFs and MYCs bound intervals and BED files for G-box and PBE boxes were visualized in Integrated Genome Browser software (IGB, http://bioviz.org/igb/)

**RT-qPCR analysis in arabidopsis**

Seven days-old plants were harvested and frozen in liquid nitrogen. RNA was extracted using a Plant total RNA purification mini kit (Favorgen®). One microgram of RNA was used for cDNA synthesis using a MultiScribe Reverse Transcriptase (Applied Biosystems). PCR was performed on a 7500 thermocycler using SYBR-green (both from Applied Biosystems). Actin was used as endogenous control.

**Western blot analysis**

Six to eight 5-days-old seedling grown in white light were harvested per sample, frozen in liquid nitrogen and homogenized in 100µl of 2X Laemmli SDS-PAGE protein loading buffer with 3% β-mercaptoethanol. Protein extracts were boiled at 90°C during 10 minutes, placed on ice during 2 minutes and centrifuged at 13000 rpm for 15 minutes at 4°C. Samples (35µl) were loaded into a SDS-PAGE gel, transferred to nitrocellulose membrane (Bio-Rad), blocked with 5% milk. Membrane was first incubated with anti-HY5 (Santa Cruz Biotechnology, dilution 1:2000) and afterwards incubated with anti-goat-HRP (Invitrogen). ACTIN was used as loading control, incubating with monoclonal anti-ACTIN (produced in mouse, Sigma-Aldrich, dilution 1:4000). Blots were developed using SuperSignal® West Pico Chemiluminescent Substrate (Thermo Scientific).

**Phylogenetic analysis**

JAZ proteins sequences from *Arabidopsis thaliana* and *Solanum lycopersicum* (tomato) were aligned with Dialing software (http://www.genomatix.de/cgi-bin/dialign/dialign.pl). Phylogenetic tree was represented using the online tool “Phylodendron”, (http://iubio.bio.indiana.edu/treeapp/treeprint-form.html).

**RT-qPCR analysis in tomato**

Leaf tissue or epidermal peels were harvested from 4 to 6 weeks-old plants and frozen in liquid nitrogen. RNA was extracted using a Plant total RNA purification mini kit (Favorgen®). One microgram of RNA was used for cDNA synthesis using a MultiScribe Reverse Transcriptase (Applied Biosystems). PCR was performed on a 7500 thermocycler using SYBR-green (both from Applied Biosystems). *SlActin* was used as endogenous control. Oligonucleotides used in this study are described in Supplemental Table 1. Data analysis shown was done using three technical replicates from one biological sample; similar results were obtained with at least two additional independent biological replicates.

**Plasmid construction**

Designed gRNAs (Supplemental Table 2) targeting the Jas domain of *SlJAZ2* were cloned into the vector Bsa_Bbs_tandem gRNA_pBS. This vector confers resistance to ampicillin and gRNAs are expressed under different versions of the ubiquitin promoter. Then, a fragment containing both gRNAs and their promoters were cloned into the vector Pk7_CAS9-TPC_polylinker pBKS. This vector confers resistance to spectinomycin in bacteria and kanamycin in plants. Cas9 is expressed under an ubiquitin promoter. Annealing of gRNAs and cloning was performed by ordinary methods using BsaI and BbsI restriction enzymes. Fragment with the two gRNAs together with their promoters were clone using the KpnI restriction enzyme. gRNAs were designed with the online tool “Breaking Cas” (Oliveros et al., 2016) (http://bioinfogp.cnb.csic.es/tools/breakingcas/). gRNAs were unique and specific for the target region (Jas domain sequence of *SlJAZ2*). 1º gRNA had a score of 96.3% with the best possible off-targets having a 0.2%. 2º gRNA had a score of 98.4%, with the best possible off-targets having a 0.5%.

**Tomato plant growth and transformation**

A tomato cultivar *Moneymaker* was transformed with the pK7_CAS9-TPC_polylinker pBKS, containing both gRNAs for *SlJAZ2*, as previously described (Wittmann et al., 2016). Plants were grown under a 16-h-light/8-h-dark cycle in a growth chamber or greenhouse. Around 120 cotyledons (60 tomato plants) were initially used for transformation with *Agrobacterium*. Many cotyledons generated a callus and produced shots, which were transferred for root generation. In total, 23 regenerated plants were transferred to the greenhouse. PCR amplification of *SlJAZ2* and DNA sequencing identified mutations in these plants and indicated that 8/23 were wild-type, 12/23 were heterozygous or chimeras and 3/23 contained an homozygous mutation. T1 and T2 progeny of selected *Sljaz2Δjas* Lines (1 and 2) was further obtained and analyzed by DNA sequencing of *SlJAZ2* to confirm that homozygous mutations were stably transmitted to the offspring.

**Measurements of stomatal aperture**

After 2 days of stratification of seeds at 4ºC, tomato WT and *Sljaz2Δjas* Lines 1 and 2 were grown on soil in a chamber with an 8h light period at 23ºC and a 16h dark period at 19ºC, relative humidity of 75%. The abaxial side of leave from 4- to 6 week-old tomato plants were collected and stuck on cover slips (peeled). Samples were incubated in a solution of 10 mM MES/Tris pH 6.0 and 30 mM KCl (working buffer). For promotion of closure assays, compounds (10μm flg22, 10μm flg22 + 2μm COR or a mock solution) were directly diluted in the working buffer in contact with epidermal peels during 2 hours. Aperture of stomata and hydathode pores were determined under an optical microscope fitted with a camera lucida and a digitizing pad linked to a computer as described (Leonhardt et al., 1997). Values reported are the means of at least three independent experiments, for which 60 aperture widths were measured each time. Error bars represent standard deviations of the means. One-way Anova with Tukey-HSD was used for statistical analysis. Calculations were performed using a statistical calculator (http://astatsa.com/OneWay_Anova_with_TukeyHSD/).

**Pseudomonas bacterial strains**

*Pseudomonas* strains used in this study were *Pseudomonas syringae* pv. *tomato* (*Pto*) DC3000 and the coronatine-deficient *Pto* DC3000 strain (*Pto* DC3000 *COR−*) which is a *Pto* DC3000 AK87 mutant that carries mutations in cmaA (coronamic acid A) and cfa6 (coronafacic acid 6) (Brooks *et al.*, 2004).

***Pseudomonas syringae* DC3000 infection assays**

Tomato plants for infection assays were grown in a cycle of 14 hours light and 10 hours darkness with 45-60% humidity for 6-7 weeks. Bacterial growth assays in tomato were performed as described previously with some modifications (Balmuth and Rathjen, 2007). For surface infection assays, plants were dipped in a bacterial suspension containing $10^8$ colony-forming units $mL^{-1}$ (cfu/ml) bacteria ($OD_{600}$= 0.2) with 0.02% Silwet L-77. For bacterial growth assays by syringe infiltration, leaves were syringe infiltrated with a bacterial suspension containing $5x10^5$ cfu/ml bacteria ($OD_{600}$= 0.001). Leafs disks were collected two days (infiltration) or six days (surface infection) post infection and bacterial growth was quantified as described previously (Gimenez-Ibanez et al., 2009). Error bars indicate SEM (n = 7). These experiments were repeated at least three times with similar results, and representative results are shown.

***Botrytis cinerea* infection assays**

*B. cinerea* infection assays were performed as described previously (Monte et al., 2014) with some modifications. 5 to 6 week-old tomato leaves were inoculated with 20µl of a suspension of $5 \times 10^6$ spores $ml^{-1}$ PDB (Difco, Le Pont de Claix, France). At least 8 leaves were inoculated per treatment.

Disease symptoms were scored 4 days post inoculations. Area of the lesion was measured using *jimage* software (https://imagej.nih.gov/ij/). This experiment was repeated twice with similar results.

**Leaf temperature and water transpiration ratio**

For leaf temperature assays, 3 to 4 weeks tomato plants were examined under Thermacam infrared camera (FLIR A655sc 25°, 50Hz) during different days. Images were saved and analysed on a personal computer using the ResearchIR4 Max Software provided by FLIR. For the calculation of water transpiration rate, plants were stratified 2 days at 4ºC in dark and grown in soils from 1 to 2 weeks. Then plants were transferred to pots with soil at 20% humidity (all pots weight the same and humidity content was calculated to be 20%) and keep some days for acclimatization. During at least 10 days plants weight was measured every day, after measuring water was added to restore 20% humidity in pots, a control (without plant) was used to measure the amount of water lost by exchange of the soil. The difference of the water lost compare to the negative control (without plant) is a measure of the water transpiration rate of the plants through the stomata. This experiment was repeated twice with similar results.

**Statistical analysis**

Unless specified, one way Anova with Tukey-HSD was used for all statistical analysis. Error bars represent standard deviation (SD). For hypocotyl length, at least 12-20 plants were used per experiment in at least two independent biological replicates. Statistical calculations were performed using a statistical calculator (http://astatsa.com/OneWay_Anova_with_TukeyHSD/). Statistical significance based on Students´s *t* test analysis was calculated using Excel software (*$p<0.05$; **$p<0.01$).

**Experimental contributions**

I, Andrés Ortigosa Urbieta, performed all the experiments except the microarray design, hybridization and data analysis (Gloria García-Casado and José Manuel Franco, Genomics Unit, CNB-CSIC,Madrid), ChIP-Seq and data analysis (Mark Zander and Mathew Lewsey, Salk Institute, USA; and José Manuel Franco, Genomics Unit, CNB-CSIC, Madrid), design of CRISPR vectors (Michael Nicolas, Plant Molecular Genetics, CNB-CSIC, Madrid) and monochromatic light experiments (Sandra Fonseca, Plant Molecular Genetics, CNB-CSIC, Madrid). Selena Gimenez-Ibañez (Plant Molecular Genetics, CNB-CSIC, Madrid) helped me with Pseudomonas and Botrytis infections in tomato.

# RESULTS

**Chapter 1:** The JA-pathway MYC transcription factors regulate photomorphogenic responses by modulating the expression of PIF targets and HY5

### *myc* mutants show *phyB*-related phenotypes

Activation of JA-Ile signalling is associated with growth inhibition, which reduces crop yield. However, the mechanism underlying this trade-off is unknown. We previously found that light quality influences JA-mediated defences by modulating the stability of MYC2, MYC3 and MYC4 transcription factors and their JAZ repressors (Chico et al., 2014). MYCs are degraded in the dark, likely by COP1, and stabilized in the light, mainly through PhyB. The fact that MYC protein stability is regulated by light and by the phytochromes suggested that MYCs could have a role in phytochrome signalling.

We observed that a multiple *myc* mutant (*mycQ; myc2myc3myc4myc5*) had a defect in seed germination specifically in the dark, but not in the light, which is reminiscent of *phyB* germination defects (Fig 4A; (Shinomura et al., 1994)). This observation suggested that MYCs, whose stability is regulated by light and by PhyB, could act downstream of PhyB to modulate photomorphogenic responses. To test this hypothesis and to analyze the contribution of each gene, we measured hypocotyl length in single or multiple *myc* mutants under different light regimes and compared them with WT and *phyB.* Under white light conditions (WL; see methods), single *myc2* and *myc3* mutants showed a slightly longer hypocotyl than WT plants (Figure 4B). This phenotype was enhanced in triple (*mycT; myc2myc3myc4*) or quadruple (*mycQ; myc2myc3myc4myc5*) combinations (Figure 4B,C). In low light conditions (LWL; see methods), which favour hypocotyl growth, significant differences were still apparent between WT plants and quadruple, triple and *phyB* mutants (Supplemental Figure 1). Growth in continuous monochromatic Red (R), Far-Red (FR) or Blue (B) light showed a specific defect of the mutants in R light perception (Figure 4D), suggesting that MYCs are required for full PhyB-mediated responses. A minor defect was also observed in blue light (Figure 4D), which is consistent with the regulation of MYCs stability by cryptochromes (Chico et al., 2014).

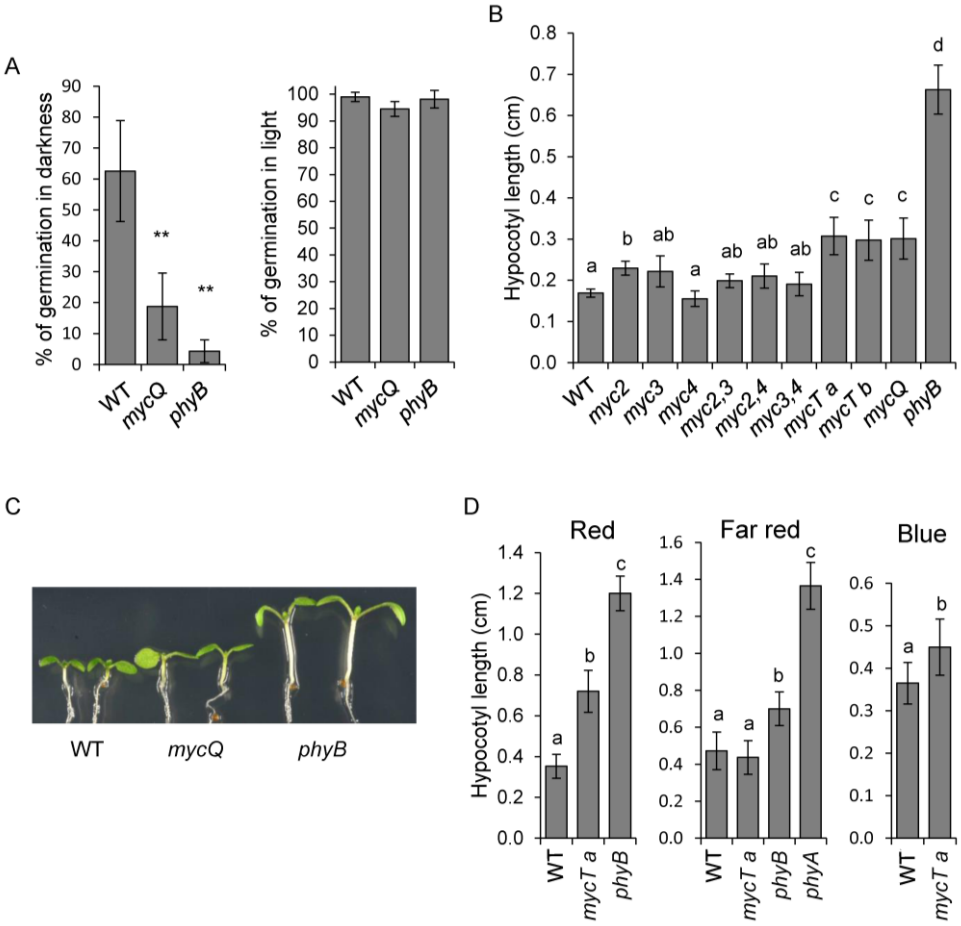


**Figure 4.** Multiple *myc* mutants show *phyB*-related phenotypes. **(A)** Quadruple *myc* mutant (*mycQ*) shows germination defects in dark but not in light, similar to that in *phyB*. **(B,C)** Hypocotyl length of WT, *phyB* and different single and multiple *myc* mutants in white light (WL) conditions. a and b in *mycT* represent two independent triple mutant lines. **(C)** *mycT* shows a defect in red light perception**.** Analysis of hypocotyl length of WT, *mycT a, phyB-9* and *phyA-211* in Red (6 days), Far-Red (7 days) and Blue (6 days) monochromatic wavelengths. Error bars represent SD. Letters above bars represent statistically distinct groups ($p<0.01$, one way Anova with Tukey-HSD). Asterisks represent significant differences * $p<0.05$, ** $p<0.01$

To further explore the hypothesis that MYCs may be required for PhyB-mediated responses, we measured hypocotyl length in plants overexpressing MYC2-GFP in WT and *phyB* backgrounds (Chico et al., 2014). In both WL and LWL conditions, MYC2 overexpression was sufficient to reduce hypocotyl growth and partially suppressed the elongated hypocotyl phenotype of *phyB* (Figure 5A,B,C,D). These results collectively indicate that MYC2, and likely the other MYC family members, are photomorphogenic regulators modulating hypocotyl growth downstream of PhyB.

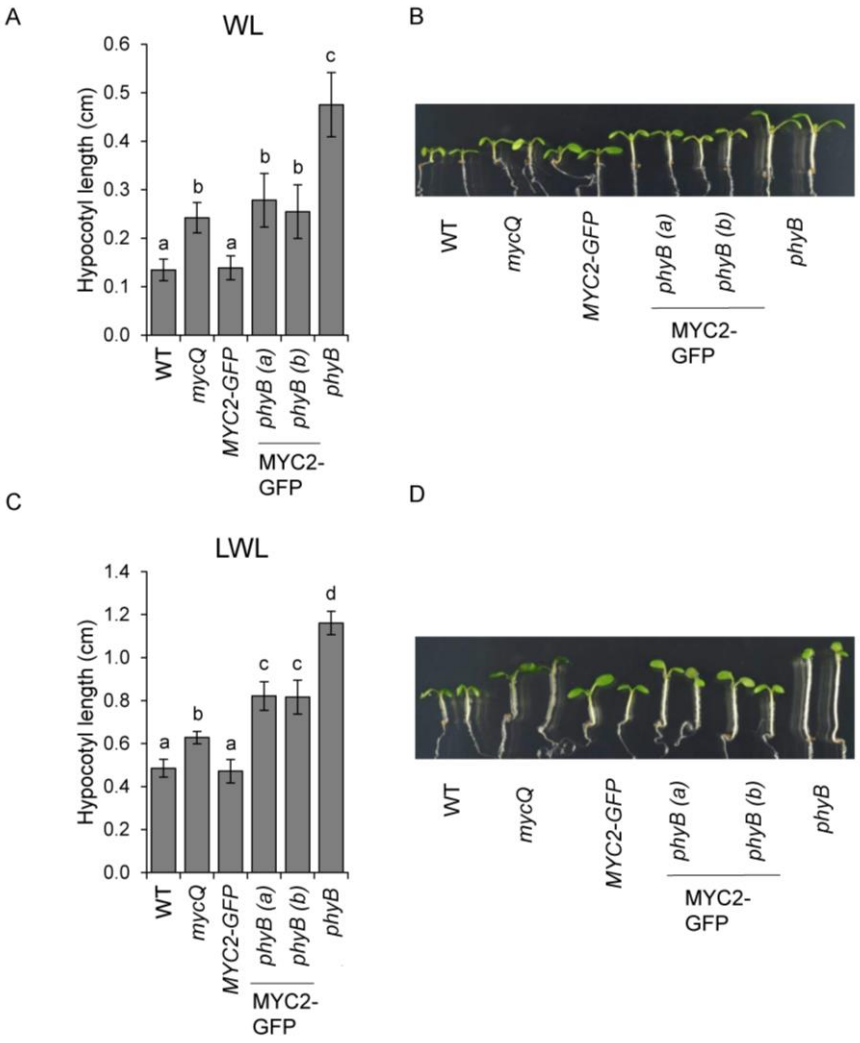


**Figure 5.** Hypocotyl length in white light (WL) **(A,B)** and low white light (LWL) **(C,D)** conditions of WT, *mycQ*, *phyB-9* and 35S:MYC2-GFP in WT and *phyB* background (a and b represent two independent lines). Error bars represent standard deviation (SD). Letters above bars represent statistically distinct groups ($p<0.01$).

**MYC photomorphogenic activity correlates with MYC levels and is partially independent of COI1**

To assess the role of JA and JA-pathway components on MYC-dependent photomorphogenesis we measured hypocotyl growth in WT and JA-related mutants treated with or without JA. Consistent with a role of MYCs in hypocotyl growth inhibition, untreated (mock) genotypes with enhanced MYC activity (35S:*MYC2* transgenics or *jazQ* mutants) had shorter hypocotyls than untreated WT plants in LWL (Figure 6; differences in WL were not statistically significant, Supplemental Figure 2). Moreover, JA treatment, which stabilizes MYC proteins (Chico et al., 2014), also promoted a reduction in hypocotyl length in WT plants (Figure 6). This JA-triggered reduction was more pronounced in 35S:*MYC2* transgenics or *jazQ* mutants grown under LWL or WL (Figure 6 and Supplemental Figure 2).

Therefore, hypocotyl length correlated well with MYC protein activity suggesting that MYCs are necessary and sufficient for hypocotyl growth inhibition. Interestingly, JA treatment also reduced hypocotyl growth in *mycQ* and *coi1-30* (a strong allele of *coi1*), albeit to a lesser extent than in WT (33% in WT vs 18% in *mycQ* and 19% *coi1-30*; Figure 6). These results indicate that exogenous JA treatment has an additional effect on hypocotyl growth inhibition that is partially independent on MYCs and COI1. Another striking observation is that in the absence of hormone treatment, hypocotyls of *coi1-30* were not significantly different from those of WT, in contrast to those of *mycQ*. We conclude that MYCs have a photomorphogenic role in hypocotyl elongation that is partially independent of COI1, and that JA has two effects on hypocotyl growth inhibition, one through the stabilization of MYCs and another independent of MYCs and COI1.

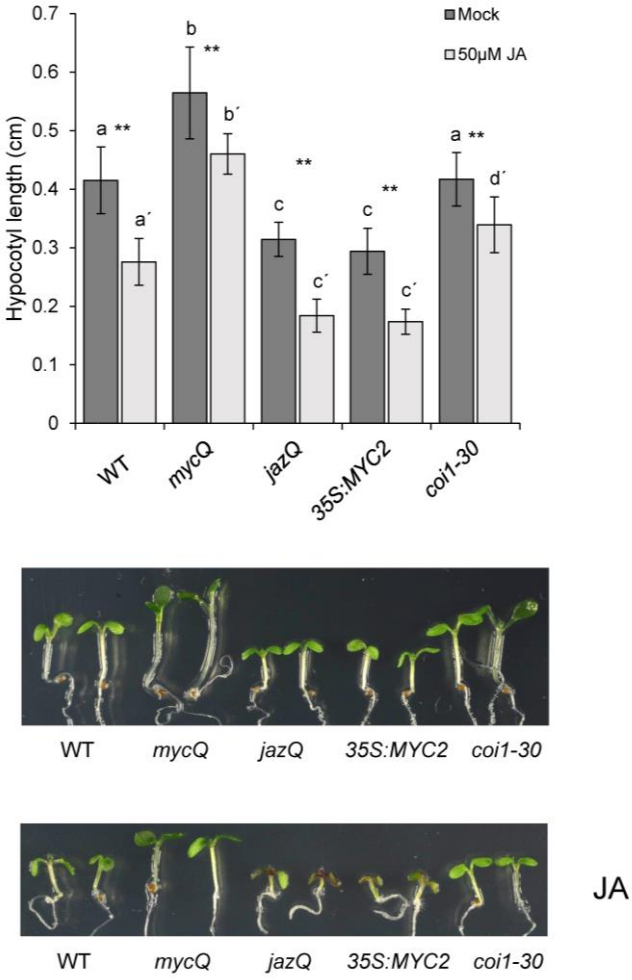


**Figure 6.** MYC photomorphogenic activity is partially independent of JA and the JA-pathway. Hypocotyl length of WT, *mycQ*, *jazQ*, 35S:MYC2 and *coi1-30* in low white light (LWL) conditions. Error bars represent SD. Letters above bars represent statistically distinct groups ($p<0.01$) among mock samples or among JA treated samples. Asterisks represent significant differences between the two conditions of a genotype ($p<0.01$).

**The COI1-independent effect of JA is dependent on interference with auxin response**

Auxins act downstream of light signalling and are ultimately responsible for hypocotyl growth (Franklin et al., 2011; Hornitschek et al., 2012). Exogenous JA treatment can lead to the formation of JA-conjugates such as JA-Trp that inhibit auxin responses through the inhibition of TIR1-mediated signalling and/or AUX1-mediated auxin transport (Staswick, 2009; Staswick et al., 2017). To test if JA-triggered inhibition of hypocotyl growth depends upon the auxin response, we analyzed the effect of JA on the triple auxin receptor mutant *tir1,afb2,afb3*. The hypocotyl of this mutant was shorter than that of WT and had a reduced response to JA (Figure 7A), thus suggesting that JA may act to suppress or interfere with auxin perception. Supporting this conclusion, the simultaneous treatment of WT plants with JA and/or the auxin transport inhibitor NPA showed that inhibition of auxin transport reduces hypocotyl length and makes the seedling insensitive to exogenous JA (Figure 7B). Therefore, we conclude that the effect of exogenous JA treatment on hypocotyl length is due to interference with auxin homeostasis (transport or perception), likely through the conversion of JA into conjugates such as JA-Trp (Staswick, 2009; Staswick et al., 2017).

To understand whether the *mycQ* photomorphogenic phenotype could also be due to auxin homeostasis we treated *mycQ* with NPA and measured hypocotyl growth. As shown in Figure 7C-D, NPA reduced the hypocotyl length of *mycQ,* similar to its effect on WT plants in both WL and LWL conditions. However, the length of *mycQ* hypocotyls after NPA treatment was still greater than that of WT. This result suggests that the elongated hypocotyl of *mycQ* is, at least in part, unrelated to auxins.

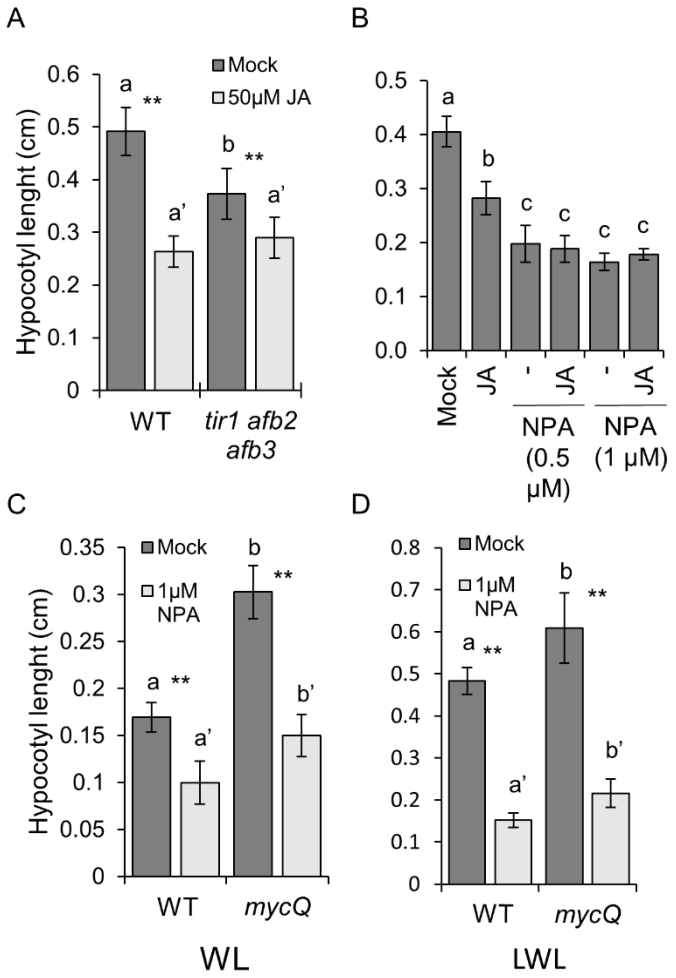


**Figure 7.** Exogenous JA interferes with auxin homeostasis. **(A)** Hypocotyl length of WT and triple auxin receptor mutant *tir1afb2afb3* in low white light (LWL) conditions. **(B)** Effect of auxin transport inhibitor naphthylphthalamic acid (NPA) on JA-mediated inhibition of hypocotyl growth of WT in LWL conditions. **(C, D)** Effect of NPA on hypocotyl growth of WT and *mycQ* in white light (WL) **(C)** and LWL **(D)** conditions. In spite of reduction, *mycQ* hypocotyls remain larger than WT. Error bars represent SD. Letters above bars represent statistically distinct groups ($p<0.01$). Asterisks represent significant differences between the two conditions of a genotype ($p<0.01$).

**Effect of MYCs and JA in photomorphogenesis is independent on DELLAs**

To understand the mechanism by which MYCs regulate photomorphogenesis, we first analyzed the effect of MYCs on PIF activity by a possible indirect effect of MYCs on the JAZ-DELLA interaction. Mutual repression of JAZ and DELLA has been proposed as a mechanism to balance growth and defence (Hou et al., 2010; Yang et al., 2012; Chini et al., 2016). In the absence of JAZ, DELLAs would be fully active, repressing PIF transcription factors and inhibiting growth. In contrast, when the levels of JAZ are high, they will repress DELLAs favouring PIF activity and hypocotyl growth. We hypothesized that in the absence of MYCs there might be more JAZ available for repressing DELLA, and therefore, the elongated hypocotyl in *mycQ* could be a consequence of a higher PIF activity. To

test this hypothesis we treated quintuple *della* mutants with JA, which promotes JAZ degradation, and found that the hormone reduced hypocotyl growth to a similar extent in quintuple *della* as in WT plants (Figure 8A,B). Indeed, the growth inhibition in WL was even greater in *della* than in WT. This result suggested that the putative excess of JAZ in *mycQ* and their interaction with DELLAs cannot explain the elongated phenotype of the *myc* mutants. This is consistent with the previous observation that the effect of exogenous JA is mostly dependent on interference with the auxin response and independent of DELLAs.

Next, we analyzed the effect of modulating DELLA protein levels by treatments with GA, which promotes DELLAs degradation, or Paclobutrazol (PACLO), which inhibits GA synthesis and stabilizes DELLAs (Rademacher, 2000; Mcginnis et al., 2003; Dill et al., 2004). As predicted, GA stimulated hypocotyl growth in all genotypes analyzed except in the quintuple *della* (Figure 8C). In WT plants, GA increased hypocotyl length similarly to that of *della* mutants. However, in the case of *mycT* or *mycQ* mutants the growth stimulation was significantly stronger, reaching a length higher than that of quintuple *della.* This demonstrates that the elongated phenotype in these *myc* mutants is not a mere consequence of DELLA inhibition by a putative excess of JAZ, and suggests that this phenotype depends on an effect of MYCs in another process independent of DELLAs.

Phenotypes of *coi1* alleles were indistinguishable from those in WT plants further indicating that the elongated hypocotyl in *myc* mutants occurs independently of COI1 function.

PACLO treatment reduced hypocotyl length in all genotypes, except in quintuple *della* (Figure 8D). However, the final length of *mycT* and *mycQ* mutants was still greater than that of WT, a further indication that the elongated phenotype in *myc* mutants is, at least partially, independent of the levels of DELLAs (Figure 8D).

Finally, we analyzed the role of DELLAs in the germination defect of *mycT*. RGL2 is a repressor of germination (Lee et al., 2002). The germination rate in the dark of *rgl2* was increased relative to WT, whereas the triple *myc* mutant had a reduced germination relative to WT. Quadruple mutants *mycT rgl2* had a germination rate in the dark similar to that of *mycT*, indicating that *mycT* is epistatic over *rgl2* and that MYCs act downstream RGL2/DELLAs (Figure 8E).

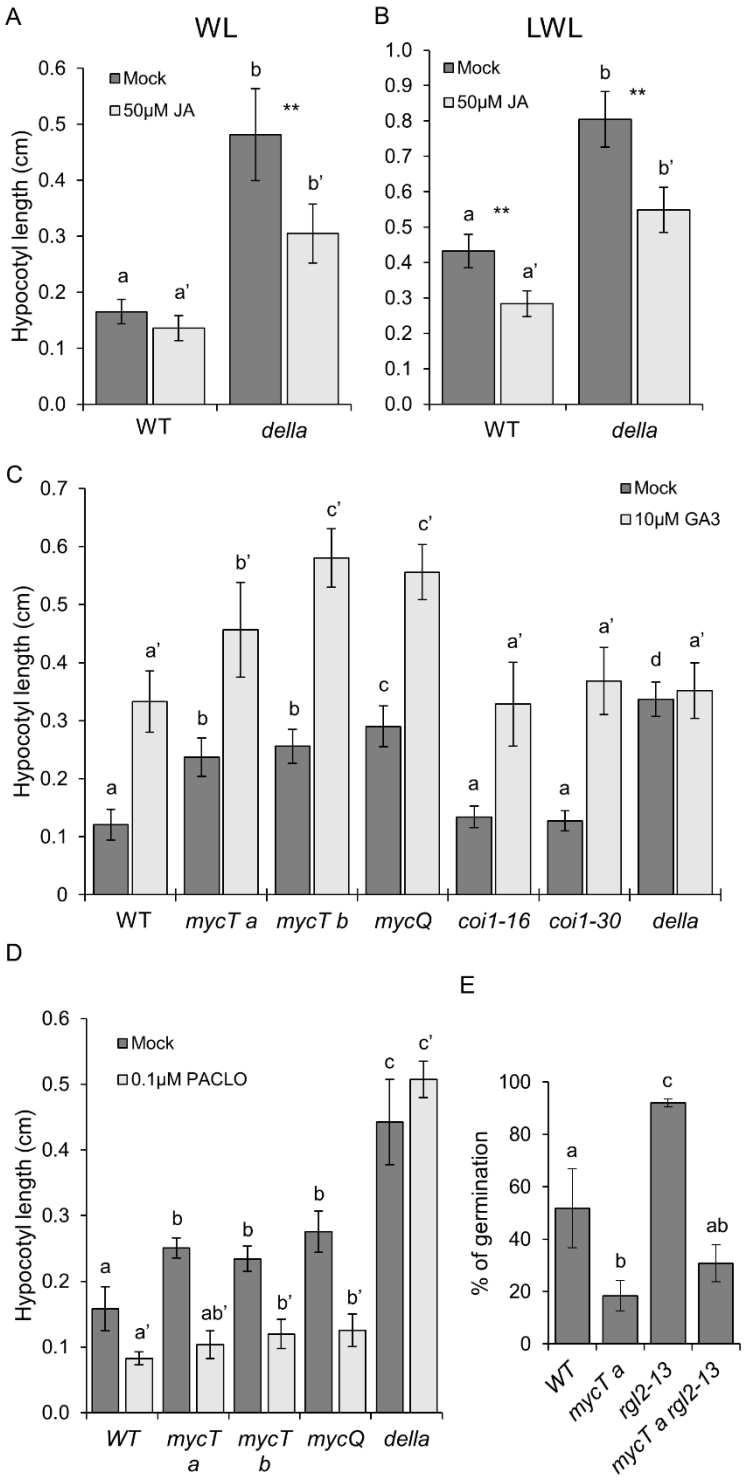


**Figure 8.** Effect of JA and MYCs in hypocotyl inhibition is independent of JAZ-DELLA interaction. Hypocotyl length of WT and quintuple *della* mutants grown with or without JA in white light (WL) **(A)** or low white light (LWL) **(B)** conditions. **(C)** Hypocotyl length of WT, *mycT a*, *mycT b*, *mycQ*, *coi1-16*, *coi1-30* and quintuple *della* treated or not with giberellin (GA3) under white light. **(D)** Hypocotyl length of WT, *mycT a*, *mycT b*, *mycQ* and quintuple *della* plants grown with or without paclobutrazol (PACLO) under white light. **(E)** *mycT* is epistatic over *rgl2*. Germination in dark of WT, *mycT a*, *rlg2-13* and *mycT rgl2*. Error bars represent SD. Letters above bars represent statistically distinct groups ($p<0.01$). Asterisks represent significant differences between the two conditions of a genotype ($p<0.01$).

**MYCs are required for R-light induced gene expression**

Once we had determined that the photomorphogenic phenotypes of *myc* mutants were not related to DELLAs, we sought to identify other targets of MYCs by transcriptomic analyses of *mycT* mutants. Since MYCs are stabilized by R light and destabilized by FR light (in a PhyB-dependent manner) we compared *mycT* vs WT plants grown under WL and either subjected or not to 3h FR-supplemented WL treatment to inhibit PhyB-mediated (and MYC-mediated) gene expression. We also meta-analyzed the differentially expressed genes (Fold-change ≥2 or ≤-2 and FDR<0.05), comparing them with available light-related transcriptomic data (Figure 9A). Among genes differentially down-regulated in *mycT* compared to WT grown in WL, more than half (clusters 1 and 2) were genes positively regulated by R light, (RL 1h; RL 2d) and negatively regulated by FR light (FR 1h; FR 3h). This regulation is particularly clear in cluster 1, but also appreciable in cluster 2. Consistent with the destabilization of MYCs by FR, most genes in clusters 1 and 2 were not differentially regulated when plants were subjected to 3h FR treatment (lane *mycT* FR). GO analyses of these genes showed their involvement in R, FR and UV light signalling (Supplemental Table 1). This data suggested that MYCs regulate (PhyB-dependent) R-light responsive genes, which are downregulated by FR.

Remarkably, genes in cluster 1 were also down-regulated in *hy5* mutants, a trend also appreciable in cluster 2, and included the *HY5* gene itself. HY5 is a classical regulator of photomorphogenesis and, therefore, its down-regulation in *myc* mutants is a likely causal effect of their photomophogenic phenotype.

We also found a set of genes downregulated in *mycT* both in WL and FR (clusters 3 & 4). In this case, expression of these genes was not defective in *hy5* mutants, suggesting that MYCs modulate expression of light-regulated genes also by a mechanism independent of HY5. Comparison of differentially expressed genes in *mycT* with available transcriptomic data of *pif* mutants revealed that genes downregulated in *mycT* (clusters 1 to 5) tend to be upregulated in different *pif* mutants (Figure 9A). These data suggested that MYCs and PIFs share an antagonistic regulation of targets genes. Strikingly, MYCs and PIFs both belong to the bHLH family of TFs and they recognize related DNA-binding motifs, the G-box and G-box variants AACGTG or CATGTG (also called PBE, PIF Binding Element) in the case of MYCs and the G-box and PBE in the case of PIFs (Godoy et al., 2011; Fernández-Calvo et al., 2011; Hornitschek et al., 2012; Zhang et al., 2013; Franco-Zorrilla et al., 2014). This strongly suggests that they might antagonize each other directly.

Analysis of the promoters of genes in clusters 1 to 6 for the presence of the MYC binding site (G-box and the G-box variants CATGTG and AACGTG; (Godoy et al., 2011; Fernández-Calvo et al., 2011)) revealed a significant overrepresentation of these target sites in several clusters (Supplemental Figure 3). Strikingly, both G-box variants were also present in the promoter of *HY5*, suggesting that it may

be a direct target of MYCs. In contrast to HY5, PIF genes were not differentially expressed in *mycT* (Supplemental Figure 4), thus excluding a mere direct regulation of MYCs on PIFs expression, and rather suggesting that MYCs and PIFs might regulate shared targets antagonistically.

In summary, the transcriptomic analysis of *mycT* mutants showed that MYCs are regulators of R-light responsive genes and suggested two possible mechanisms of action: regulation of HY5 expression and/or PIFs activity.

### ***HY5*** **is a direct transcriptional target of MYCs**

To address if *HY5* or *PIFs* could be direct transcriptional targets of MYCs, we performed chromatin immunoprecipitation sequencing (ChIP-Seq) in transgenic *A. thaliana* plants expressing MYC2:GFP or MYC3:GFP under their native promoters (Zander, Lewsey, Ecker and colleagues, *unpublished*; see Methods). A significant enrichment of reads ($p < 1e\text{-}25$ and present in three biological replicates) was found in the promoter region of *HY5* from both MYC2 and MYC3 ChIP-Seq, centered at approximately 150 bp upstream of the TSS and coincident with a G-box like (PBE) sequence at this position (Figure 9B; see Supplemental Figure 3D). This finding, together with reduced expression of *HY5* in the *mycT* genotype indicated above, suggests that *HY5* is a direct transcriptional target of MYCs. To further confirm these results, we analyzed transcript and protein levels in *mycT* and *mycQ.* We observed that *HY5* transcript levels were reduced in *mycT* and *mycQ* mutants compared to WT (Figure 9C), confirming that *HY5* expression is regulated by MYCs. Additionally, these lower transcript levels correlated well with lower HY5 protein accumulation in the mutant (Figure 9D). Altogether, these data indicate that MYC-dependent regulation of R-light responsive genes occurs, at least in part, through direct transcriptional activation of HY5 expression.

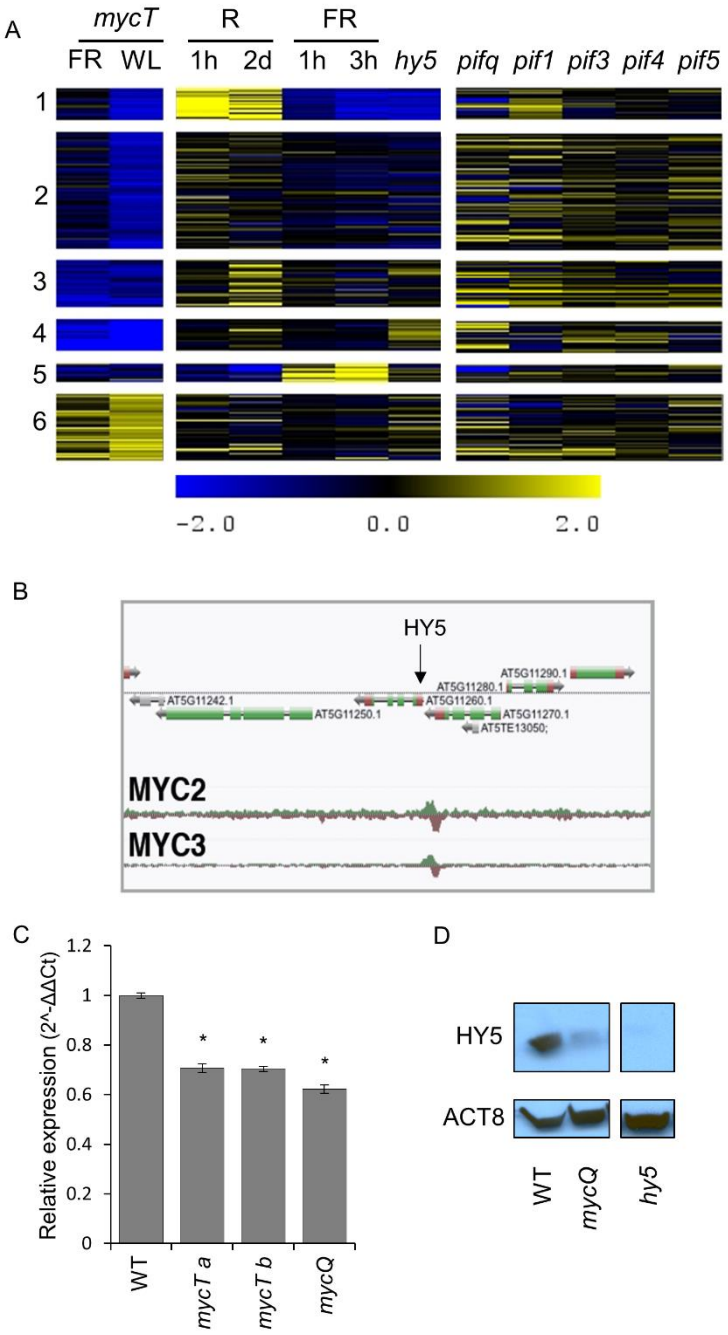


**Figure 9.** MYCs are required for Red-light-dependent gene expression and HY5 transcription. **(A)** Cluster analysis of differentially expressed genes in *mycT* vs WT grown in WL or WL supplemented with Far-Red (FR; 3h) and comparison with expression levels of the same genes in available data of Red light (R), FR, *hy5* or individual or quadruple (*pifq*) *pif* mutants. **(B)** MYC2 and MYC3 TFs directly bind to the *HY5* promoter. Representation of ChIP-Seq data showing peaks of MYC2 and MYC3 DNA-bound fragments in the promoter of *HY5.* **(C)** Q-PCR analysis of *HY5* expression in WT and multiple *myc*. Data representation was done using three technical replicates from one biological sample; similar results were obtained with two additional independent biological replicates. Error bar represent SD. Asterisks represent significant differences * $p<0.05$. **(D)** Western blot analysis of HY5 protein accumulation in WT and *mycQ*. Similar results were obtained using at least three independent biological replicates.

**MYCs and PIFs share direct targets**

As outlined above, an alternative mechanism for MYC regulation of R-light genes would involve antagonistic activity of MYCs and PIFs on shared target genes. We therefore used available ChIP-Seq data for PIFs to examine if they might share targets with MYCs. Strikingly, the numbers of target genes shared by MYC2 or MYC3 with several PIFs (PIF1, PIF3, PIF4 and PIF5) were very high, representing 3.3- to 4.2-fold for MYC2 and 3.6- to 4.2-fold enrichment for MYC3 in shared targets compared with their expected common targets ($p<10E-100$, chi sq; Supplemental Figure 5). Among shared target genes, the actual peaks bound by MYCs and PIFs were coincident or overlapping in a large proportion of them, ranging from 43 to 50% in the case of MYC2 and from 52 to 57% for MYC3 (Figure 10 and Supplemental Figure 5 and 6). Moreover, expression of a subset of these shared direct targets was differentially affected in *mycT* and *pif* mutants (Figure 9A). As shown in Supplemental Figure 7, all the clusters in Figure 9A had a significant overrepresentation of direct MYC targets ($p<0.05$), compatible with over-representation of MYC-bound sequences. Remarkably, clusters 1 and 3 showed a significant overrepresentation of direct PIF targets ($p<0.05$), indicating that these genes would correspond to shared MYC/PIF targets. Interestingly, most of the common targets of clusters 1, 3 and 5 (4/5, 4/4 and 3/3, respectively; Supplemental Figure 6) also share the same genomic interval and thus, identical bound sequences, suggesting that MYCs and PIFs may antagonize each other directly through binding identical sites.

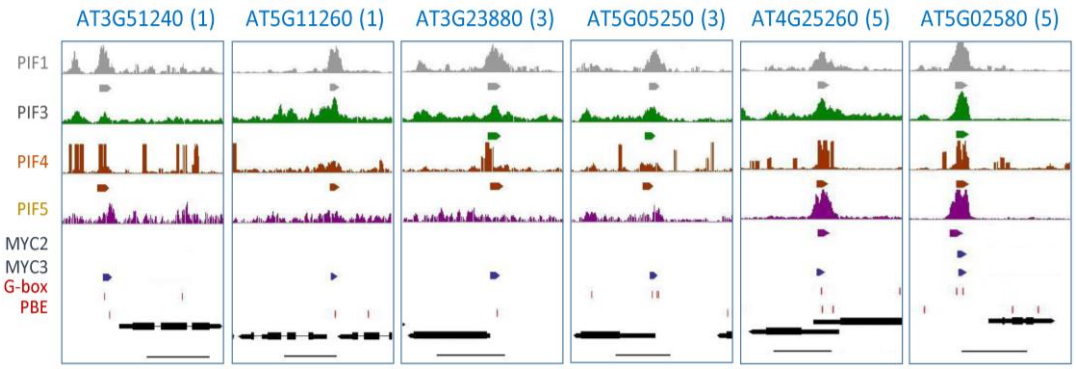


**Figure 10. Examples of PIFs and MYCs targets with shared bound sites.** Genome Browser captures of some representative genes from clusters 1, 3 and 5 showing PIFs and MYCs shared bound fragments determined by ChIP-Seq. High confidence PIF- and MYC-bound intervals are represented as colored arrows in each track. The position of PIF/MYC binding sequences G-box (CACGTG) and PBE (CATGTG) is also indicated in red. Horizontal bars correspond to 1 kb.

**-Chapter 2**: Design of a bacterial speck resistant tomato by CRISPR/Cas9-mediated editing of SlJAZ2

The antagonism between JA and SA pathways generate a defence trade-off that difficult the generation of broad-spectrum resistance by manipulation of JA or SA pathway genes.

In Arabidopsis, MYC function is required for stomatal opening by bacterially produced COR during Pseudomonas infection (Gimenez-Ibanez et al., 2017). Inhibition of MYC function impairs stomatal opening by bacterially produced COR and increases plant resistance to bacterial infection. In spite of the relevance of this role of MYCs in stomatal dynamics, the fact that MYC genes are not only expressed at the stomata guard cells but are also broadly expressed in other plant tissues prevented their biotechnological use since depletion of MYC function would reduce plant defences against necrotrophic pathogens. Modulation of MYC activity only at stomata guard cells is feasible by manipulating the MYC repressor JAZ2, which is mainly expressed at guard cells (Gimenez-Ibanez et al., 2017). In this chapter we exploited this knowledge obtained in the model plant Arabidopsis thaliana to develop a biotech tool that confer broad-spectrum resistance to crop plants. We aimed to confirm the conservation of the MYC-JAZ2 role in stomatal dynamics in tomato and edit the JAZ2 repressor using the CRISPR-Cas9 system to inhibit MYC function specifically at stomata.

**SlJAZ2 is the ortholog of AtJAZ2**

The AtJAZ2 protein belongs to the TIFY super-family that includes 12 canonical members in Arabidopsis. Similarly, twelve JAZ proteins have also been identified in tomato (Sun et al., 2011; Ishiga et al., 2013; Chini et al., 2017). However, correlation between specific versions of *JAZ* genes among plant species is unclear. In order to identify the ortholog of AtJAZ2 in tomato we performed phylogenetic analysis using protein sequences of all JAZs from both plant species. AtJAZ2 protein grouped into a clade that included AtJAZ1, and the SlJAZ1 and SlJAZ2 proteins as the closest tomato orthologues (Figure 11A and Supplemental Figure 8). SlJAZ3 and SlJAZ4 were also closer to AtJAZ2 than to any other tomato or Arabidopsis protein. Among proteins in this clade, AtJAZ1, AtJAZ2 and SlJAZ2 showed a remarkable similar length (Figure 11A). This phylogenetic analysis indicated that the ortholog of AtJAZ2 in tomato was likely SlJAZ2 or SlJAZ1, although SlJAZ3 and SlJAZ4 cannot be discarded.

*JAZ2* is strongly expressed at stomatal guard cells compared to other *JAZ*s in Arabidopsis (Gimenez-Ibanez et al., 2017). Thus, we next analyzed if any of the closest tomato candidate orthologues of *AtJAZ2* were expressed at the stomata. To do this, we performed quantitative RT-PCR analyses that compared the expression levels of these genes between tomato whole leave tissue and epidermal peels, which are enriched in guard cells. Sl*JAZ2* was the only gene enriched in the stomata-abundant epidermal peels fraction whereas Sl*JAZ1*, Sl*JAZ3* and Sl*JAZ4* relative levels were similar among them (Figure 11B). This pinpointed *SlJAZ2* as the functional tomato ortholog of AtJAZ2.

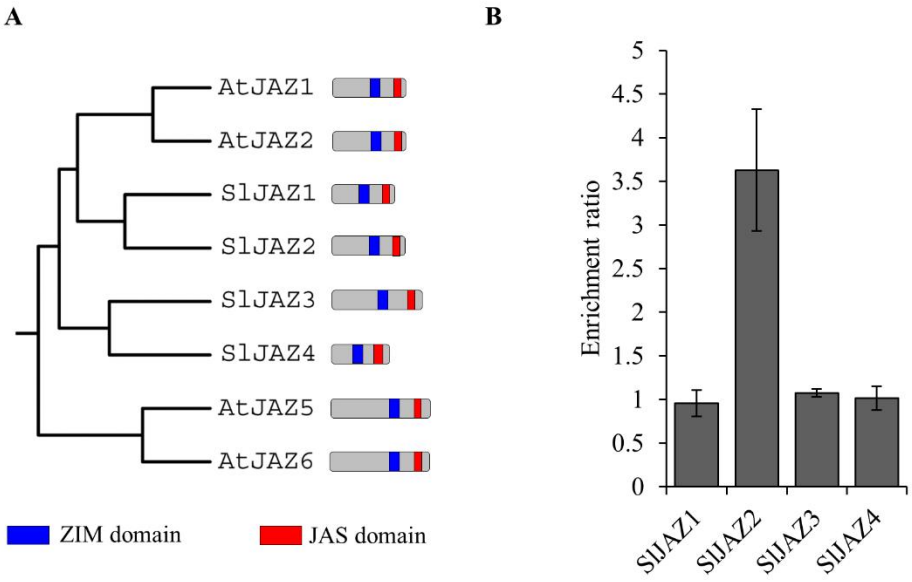


**Figure 11. SlJAZ2 is the ortholog of AtJAZ2.**
**(A)** Phylogenetic tree of JAZ1, JAZ2, JAZ3 and JAZ4 from Arabidopsis and tomato. SlJAZ1 and SlJAZ2 are the closest proteins to AtJAZ2. The schematic representation indicates length and domains of each JAZ protein. (B) Enrichment ratio of RT-PCR analyses comparing expression levels of *SlJAZ1*, *SlJAZ2*, *SlJAZ3* and *SlJAZ4* in tomato whole leave tissue and epidermal peels, which are enriched in guard cells. This experiment was repeated twice with similar results.

### *SLJAZ2* editing through CRISPR/Cas9

In Arabidopsis, a truncated form of AtJAZ2 lacking the Jas domain (AtJAZ2ΔJas) is resistant to AtCOI1-dependent degradation after COR treatment. Arabidopsis plants overexpressing this degradation resistant JAZ2 dominant form are insensitive to the phytotoxin COR and more resistant to DC3000 (Gimenez-Ibanez et al., 2017). We used CRISPR/Cas9 genome-editing technology to generate sequence-specific mutations that would disrupt the Jas domain of SlJAZ2, leading to a *JAZ2ΔJas* tomato variant in the commercial variety Moneymaker. To do this, we targeted the start site of the Jas domain in the *SlJAZ2* locus using a dual gRNA strategy that facilitates the generation of homozygous deletions (Brooks et al., 2014). The two selected gRNA targets within SlJAZ2 were positioned on opposite DNA strands, and overlapped 7 nucleotides (Figure 12A). DNA sequence analysis of primary transformants identified two homozygous lines for *SlJAZ2* containing deletions of seven and four nucleotides in the designated area (Figure 12B). Both deletions were predicted to disrupt the Jas domain of *SlJAZ2* (Figure 12B). We further explored if these genome edited *Sljaz2Δjas* mutations were specifically being expressed in our tomato lines. To do this, we performed quantitative RT-PCR experiments amplifying wild-type (WT) *SlJAZ2* or each one of the two specific *Sljaz2Δjas* mutations generated in both tomato lines. WT, Line 1 and Line 2 amplified exclusively their expected transcripts (Figure 12B), indicating both lines carry homozygous mutations at the *SlJAZ2* locus generating forms of *SlJAZ2Δjas* that are effectively being transcribed. Further analysis of T1 and T2

*Sljaz2Δjas* lines by DNA sequencing of *SlJAZ2* showed that the homozygous mutations were stably transmitted to the offspring.

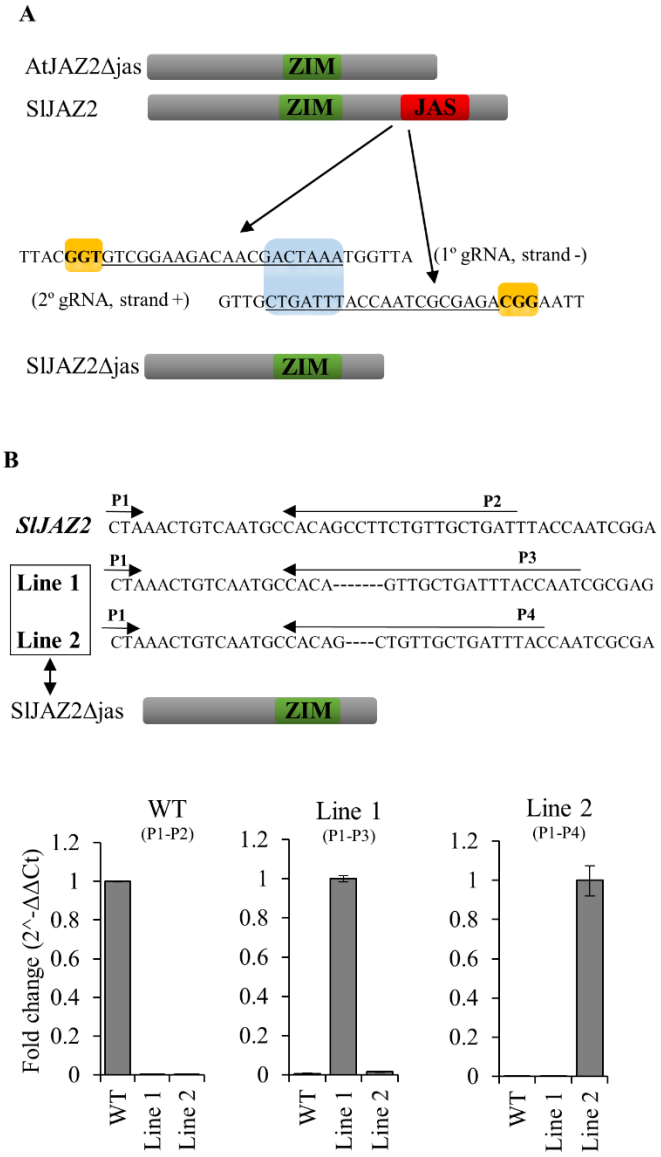


**Figure 12. CRISPR/Cas9-mediated editing of *SlJAZ2*.**
**(A)** Schematic representation of AtJAZ2Δjas, SlJAZ2, SlJAZ2Δjas, and position of both gRNAs designed to target the Jas domain in the *SlJAZ2* locus. Nucleotide sequence indicates double strand DNA of *SlJAZ2*. Yellow boxes indicate the PAM sequence. Underlined sequence indicates the two gRNAs used. The 1º gRNA is targeted before the start of the Jas domain (strand -) while the 2º gRNA is targeted to the beginning of the Jas domain (strand +). The target area of both gRNAs overlaps seven nucleotides (blue box). **(B)** Transcriptional expression by RT-PCR of SlJAZ2 and *SlJAZ2Δjas* forms in WT and *SlJaz2Δjas* plants (Line 1 and Line 2) using different combinations of primers as described in the figure.

**Gain-of-function *Sljaz2Δjas* forms prevent stomatal reopening by COR**

Pathogen perception induces stomatal closure to limit pathogen penetration. Some *P. syringae* strains produce COR as a critical virulence strategy to re-open stomata and cause disease. Thus, we next evaluated the ability of both *Sljaz2Δjas* tomato lines to close stomata upon perception of the highly conserved flg22 peptide of bacterial flagellum (Chinchilla et al., 2007), and to reopen them in the presence of COR. We incubated leaves of WT plants and *Sljaz2Δjas* mutants with flg22, flg22 plus COR or a mock solution as a control. In mock conditions, the aperture range of the stomata was wide and similar between WT and both *Sljaz2Δjas* tomato lines. As expected, flg22 induced stomatal closure in all tomatoes, whereas COR induced stomatal re-opening in WT plants (Figure 13A). In contrast to WT, both *Sljaz2Δjas* tomato lines were fully impaired in COR-mediated stomatal reopening (Figure 13A). This indicates that, similar to Arabidopsis, SlJAZ2 has a key role regulating stomata dynamics in response to bacteria and that COR-induced stomata reopening requires inhibition of *SlJAZ2,* which can not be achieved in the dominant *Sljaz2Δjas* mutants.

Stomata are the major regulators of water transpiration in plants (Brodribb and McAdam, 2017). We next evaluated whether the rate of transpiration was affected in *Sljaz2Δjas* lines compared to WT tomato plants. Time-course measurements showed that the rate of water loss in all plants was similar (Figure 13B). We also analyzed leaf temperature, which is an indirect measure of stomata opening and water transpiration, by using infrared thermography and found no differences related to stomatal apertures (Figure Supplemental Figure 9). Overall, this indicates that *Sljaz2Δjas* tomato lines are not affected in the aperture of the stomata during the process of transpiration, but are rather specifically affected in the response to bacteria.

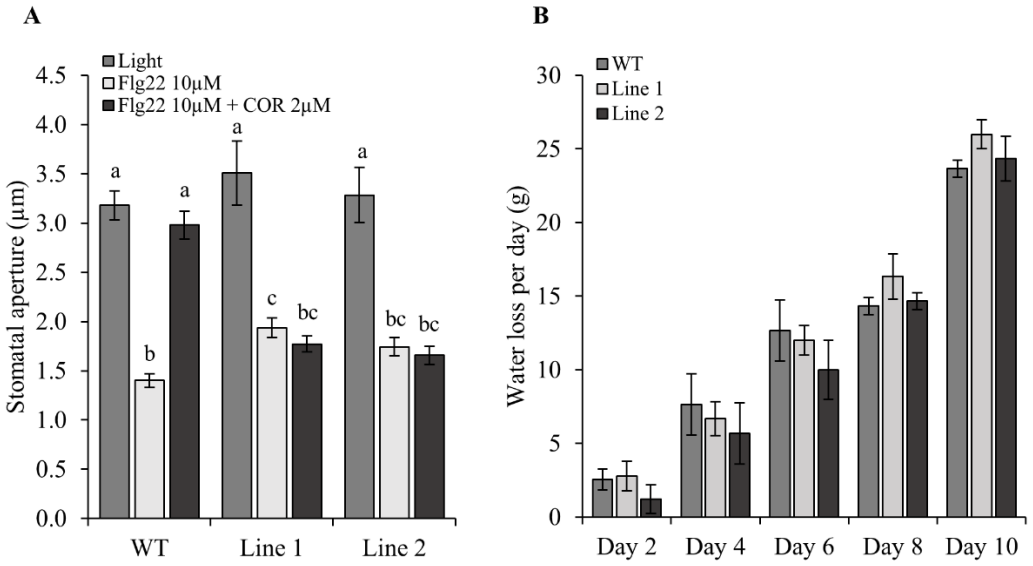


**Figure 13. *Sljaz2Δjas* mutants prevent stomatal reopening by COR.**

**(A)** Stomatal aperture in tomato WT and *Sljaz2Δjas* mutants (Line 1 and Line 2) after 2h of incubation with flg22, flg22 plus COR or a mock control. Error bars indicate standard error of the mean (SEM;

n=60). Letters above bars represent statistically distinct groups (p<0.01, one way Anova with Tukey-HSD). Similar results were obtained in three independent biological replicates **(B)** Water transpiration rate (water loss) in WT and *Sljaz2Δjas* (Line 1 and Line 2) tomato plants during a time course experiment of 10 days. Error bars indicate standard deviation (SD; n=3). Not statistical difference was found between WT and mutant lines (one way Anova with Tukey-HSD). Results are representative of two independent experiments.

### Dominant *Sljaz2Δjas* mutants are resistant to *P. syringe* infection

In order to evaluate the resistance of adult *Sljaz2Δjas* plants towards bacterial pathogens such as *P. syringae*, we next compared bacterial replication of *Pto* DC3000 on WT and both *Sljaz2Δjas* lines infected by surface inoculation (dipping) or syringe infiltration. Surface infection mimics natural infection conditions and it is a very common technique to assess plant resistance to pathogens (Zipfel et al., 2004). In contrast, the infiltration technique overcomes the early stomatal level of regulation measuring mainly apoplastic cell-based defenses. WT plants infected by surface inoculation with *Pto* DC3000 showed extensive chlorosis and specks, typical symptoms of the bacterial speck disease in tomatoes (Figure 14A). In contrast, *Sljaz2Δjas* plants did not display these typical symptoms of disease suggesting their enhanced resistance (Figure 14A). Disease symptoms correlated well with bacterial titers. *Sljaz2Δjas* plants surface inoculated showed significantly lower bacterial titers than those in its respective WT control plants (Figure 14B). In the case of plants infected with *Pto* DC3000 by infiltration, bacteria grew to similar levels on both WT and *Sljaz2Δjas* lines (Figure 14C). Consistently, inoculation with the coronatine-deficient *Pto* DC3000 strain AK87 (*Pto* DC3000 *COR*−) showed similar bacterial titles in WT and *Sljaz2Δjas* plants (Supplemental Figure 10). These results supports the idea that SlJAZ2 is a key regulator of stomata dynamics during the penetration process of *Pto* DC3000 and indicates that *Sljaz2Δjas* plants promote bacterial resistance by blocking the action of the phytotoxin COR at the stomata.

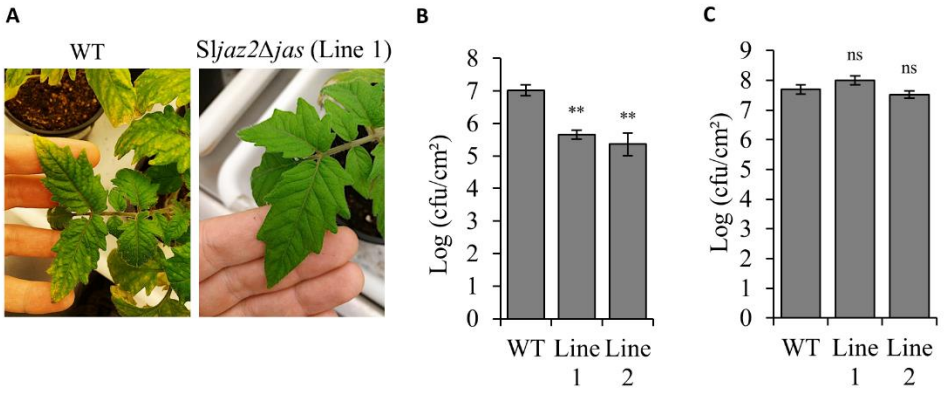


**Figure 14. *Sljaz2Δjas* mutants are more resistant to *Pto* DC3000 when surface inoculated.**
**(A)** *Pto* DC3000 disease symptoms on WT and *Sljaz2Δjas* (Line 1) tomato plants after surface inoculation with *Pto* DC3000 bacteria at $10^8$ colony-forming units $mL^{-1}$ (cfu/ml). Pictures were taken 6 days post inoculation and show typical specks caused by *Pto* DC3000. **(B)** Growth of *Pto* DC3000

on WT and *Sljaz2Δjas* (Line 1 and Line 2) tomato plants 6 days after surface inoculation by dipping with bacteria at $10^8$ cfu/ml. **(C)** Growth of *Pto* DC3000 on WT and *Sljaz2Δjas* (Line 1 and Line 2) tomato plants 2 days after syringe infiltration with bacteria at $5x10^5$ cfu/ml. Error bars indicate SEM (n=7). Asterisks represent significant differences ** $p<0.01$ (Student´s t-test). Similar results were obtained in three independent experiments and representative results are shown.

**Dominant *Sljaz2Δjas* tomato plants show unaltered levels of resistance against the necrotrophic pathogen *Botrytis cinerea*.**

The antagonism between JA and SA pathways is a barrier to improve plant immunity and generate broad-spectrum resistance. To evaluate if the insensitivity to COR generated in the edited *Sljaz2Δjas* tomato lines affects resistance against necrotrophic fungal pathogens, we selected *B. cinerea,* causal agent of the gray mold of tomatoes. Thus, we measured the susceptibility of WT and *Sljaz2Δjas* lines to *B. cinerea* by quantifying leaf infected area. Lesions caused by the fungus indicated similar progression of disease symptoms (Figure 15A) and area affected by the pathogen in WT and *Sljaz2Δjas* lines (Figure 15B). These results indicate that SlJAZ2 function seems restricted to stomata guard cells and it plays a very limited or inexistent role in apoplastic defense responses against necrotrophic fungi.

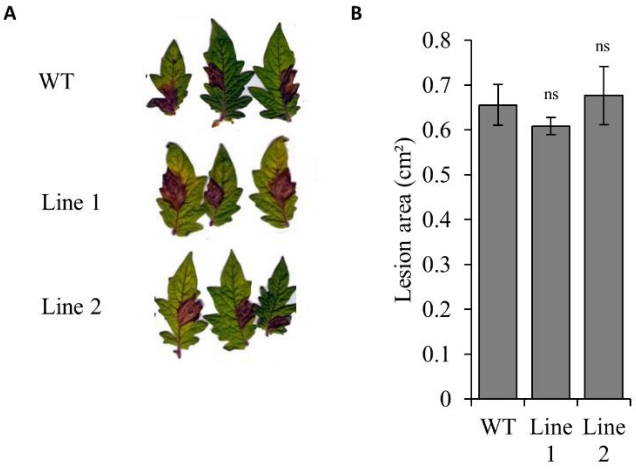


**Figure 15. *Sljaz2Δjas* mutants retain WT resistance to necrotrophic fungi.**
**(A)** *Botrytis cinerea* disease symptoms on WT and *Sljaz2Δjas* mutants 4 days post inoculation (dpi) with $5x10^6$ spores $ml^{-1}$. **(B)** Lesion Area produced by *Botrytis cinerea* on WT and *Sljaz2Δjas* mutants 4 days post inoculation (dpi) with $5x10^6$ spores $ml^{-1}$. Error bars indicate standard error SEM (n=8). (Student's t-test, $P < 0.05$; ns, not significant). Results are representative of two independent experiments.

# DISCUSSION

## The JA-pathway MYC transcription factors regulate photomorphogenic responses by modulating the expression of PIF targets and HY5

Plant fitness requires a continuous adaptation of plant growth to environmental conditions. Stress signals induce adaptive defenses at the expense of growth. Similarly, rapid growth of plants in shady canopies to reach the light dampens defences (Moreno et al., 2009; Ballaré, 2014). This growth/defence trade-off has been traditionally explained by the hypothesis that resources are limited and their allocation determines the balance between growth and defence, in the so-called “dilemma of plants to grow or to defend” (Herms and Mattson, 1992). This view has, however, been challenged by a growing body of evidence supporting the idea that signalling networks rather than resource allocation coordinate this balance to optimize fitness (Casal, 2013; Kliebenstein, 2016; de Vries et al., 2017; Guo et al., 2018). Outstanding support to this idea comes from the uncoupling of the growth/defence trade-off in the *phyB,jazQ* mutant, which is able to activate defences without sustaining a growth penalty (Campos et al., 2016). Among the different examples illustrating growth/defence trade-offs in plants (Huot et al., 2014), jasmonates have been involved in crosstalks with light, auxin and GA signalling pathways (Moreno et al., 2009; Staswick, 2009; Yang et al., 2012; Staswick et al., 2017; Zheng et al., 2017). In the case of light, red light enhances the stability of MYC proteins through a mechanism that involves COP1 inhibition by photoreceptors (mainly PhyB). Low R/FR ratios such as those in dense shady canopies, which inactivate PhyB, also destabilize MYCs and reduce JA-mediated defences (Chico et al., 2014). Therefore, MYCs are key to understanding how growth dampens defenses in the plant growth or defence dilemma (Herms and Mattson, 1992). However, if plants can defend without growth penalty, as demonstrated in the *phyB,jazQ* mutant (Campos et al., 2016), it remains difficult to understand why MYCs are destabilized in shady conditions. Moreover, how activation of defences reduces growth is still poorly understood.

In our effort to address these questions, we uncovered that defence-related MYC transcription factors are photomorphogenic regulators and targets of PhyB, which modulate the activity of other photomorphogenic factors such as HY5 and PIFs. Thus, the fact that they simultaneously regulate photomorphogenic growth and defences explains the growth/defence trade-off at the molecular level (Figure 16). In the shade, partial inactivation of PhyB (required for MYCs stability; (Chico et al., 2014)) would partially destabilize MYCs reducing HY5 protein levels and increasing activity of PIFs, therefore allowing hypocotyl growth. In these conditions, lower MYC levels and FR-mediated stabilization of JAZ repressors would reduce JA-dependent defences. Moreover, the role of MYCs in phomorphogenesis also helps to understand the uncoupling of the growth/defence trade-off in *phyB,jazQ*. The reduction of JAZ repressors in this mutant should compensate for the lower MYC levels in *phyB*, maintaining the capacity of activating defences. The lack of PhyB prevents the activity of photomorphogenic factors (including MYCs, HY5, etc) and enhances the stability of PIFs that promote hypocotyl growth. Therefore, as MYC TFs are targets of both JAZ and PhyB, their regulation

seems pivotal in fine-tuning the balance between defence and growth.

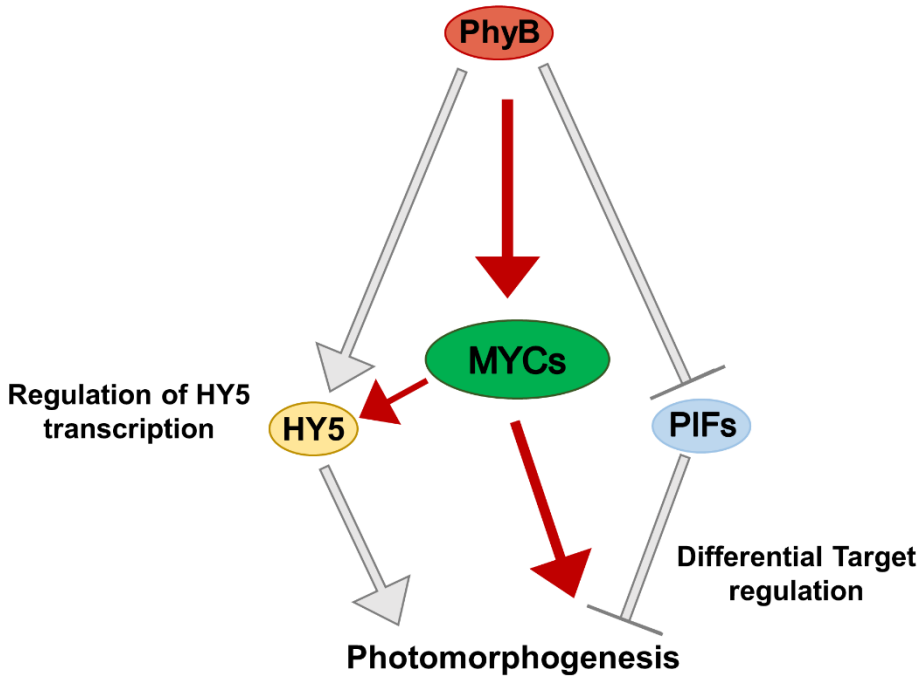


**Figure 16. Mechanistic view of MYCs role in photomorphogenesis.** Defence-related MYC transcription factors are photomorphogenic regulators acting downstream of PhyB, which modulate the activity of other photomorphogenic factors such as HY5 and PIFs. MYCs regulate photomorphogenesis by two complementary mechanisms: i) Regulation of *HY5* expression by directly binding to its promoter, and ii) opposite regulation of shared MYCs/PIFs targets. The fact that MYCs simultaneously regulate photomorphogenic growth and defences explains at the molecular level the growth/defence trade-off.

The fact that MYCs are (indirect) targets of PhyB is supported by the requirement of PhyB for stability of MYCs (Chico et al., 2014) and by the photomorphogenic phenotypes identified in multiple *myc* mutants. Thus, *mycQ* shares with *phyB* the defects in hypocotyl growth and seed germination in the dark. They also share the regulation of a set of light-regulated genes identified in our transcriptomic analyses. The photomorphogenic role of MYCs is also supported by the partial suppression of the *phyB* elongated hypocotyl by expression of MYC2 (35S:MYC2-GFP).

Transcriptomic and ChIP-Seq analyses revealed that *HY5* is a direct transcriptional target of MYC2 and MYC3 and also showed that MYCs and PIFs regulate antagonistically a subset of shared targets. This regulation may even be direct since both MYCs and PIFs recognize similar DNA-binding motifs (G-box and PBE; (Godoy et al., 2011; Fernández-Calvo et al., 2011; Zhang et al., 2013; Franco-Zorrilla et al., 2014)). These data explain mechanistically the light-related phenotypes in multiple *myc* mutants and support a role of MYCs in photomorphogenesis. Moreover, the dual-regulation of MYC-

PIF shared promoters provides a logical explanation to the surprising observation that *coi1* does not show an elongated hypocotyl as that shown by *myc* mutants. In the *coi1* background MYC proteins are still present and may bind to the shared promoters with PIFs. Since MYCs interact with a co-repressor complex that includes JAZ, NINJA and TPL, in the absence of JAZ degradation, such as that occurring in *coi1*, MYCs should behave as transcriptional repressors, thus preventing gene transactivation by PIFs. Only in the presence of COI1 and JA-Ile, would JAZ repressors be degraded by the proteasome enabling MYCs to become activators.

The role of JA in photomorphogenesis seems complex. On the one hand, exogenous JA treatment, which stabilizes MYCs (Chico et al., 2014), promotes hypocotyl shortening, an effect that is particularly clear in genotypes with an increased abundance of active MYCs, such as *jazQ* or 35S:MYC2 plants. On the other hand, only part of this effect seems to occur through the JA activation of its signalling pathway, since the exogenous treatment also promotes some reduction of hypocotyl growth in *mycQ* and *coi1-30*. Therefore, exogenous JA seems to activate photomorphogenesis by two independent mechanisms. One of them would depend on activation of MYCs, but the other appears to be independent of the JA-pathway. To understand how these two mechanisms operate, we challenged hypotheses based on previous interactions of JA and other hormonal pathways. For instance, JA has been proposed to regulate growth by interfering with GA signalling and PIFs through the JAZ-DELLA balance (Hou et al., 2010). JAZ repressors interact with and repress DELLAs; thus JAZ degradation by JA enhances DELLA function and inhibits growth (Yang et al., 2012). However, quintuple *della* mutants responded to JA similarly to WT plants, suggesting that the effect of JA on growth is independent of DELLAs. This is consistent with previous studies which show that DELLA proteins are not required for wound- and JA-induced growth stunting of leaves (Zhang and Turner, 2008). Moreover, GA promoted growth in *mycQ* to a height higher than WT or quintuple *della*, indicating that the mechanisms that induce hypocotyl growth in the quadruple *myc* add to the effect of *della*. Similarly, PACLO treatment, that stabilizes DELLAs, reduced hypocotyl growth in all genotypes, yet the length of the quadruple *myc* was still longer than that of WT, thus supporting the theory that MYCs affect a process unrelated to JAZ-DELLA interaction.

An alternative explanation for the MYC/COI-independent role of JA in hypocotyl growth inhibition is the interference with auxins. JA can conjugate with Trp and JA-Trp was shown to interfere with auxin signalling through inhibition of the auxin transporter AUX1 (Staswick, 2009; Staswick et al., 2017). Results demonstrate that the triple auxin receptor mutant *tir1afb2afb3* is almost completely insensitive to JA inhibition of hypocotyl elongation and that the auxin transport inhibitor NPA abrogates the effect of JA. These data support the theory that the MYC/COI1-independent effect of JA in hypocotyl growth is due to the interference with auxin homeostasis, likely through the effect of JA-Trp.

Finally, JA has recently been shown to repress growth in darkness by MYC2-dependent inhibition of COP1 activity and therefore HY5 stabilization (Zheng et al., 2017). The phenotype that we observe in

WL is unlikely regulated through the same mechanism, since in WL COP1 should be inactive (Von Arnim and Deng, 1994). In sunny conditions, rather than regulating COP1 activity, we propose that MYCs directly regulate the expression and, therefore, the abundance of HY5, which together with competition with PIFs for their targets explains mechanistically the role of MYCs in photomorphogenesis. Our results underscore a key role of MYCs in the growth/defence balance by showing that they are involved in the regulation of both defence and photomorphogenesis.

## Design of a bacterial speck resistant tomato by CRISPR/Cas9-mediated editing of SlJAZ2

One of the great challenges for food security in the 21st century is to improve yield through the development of disease resistant crops. However, novel strategies to improve plant immunity are particularly challenging. In vascular plants, hormonal crosstalk between JA and SA, the key two hormonal pathways controlling resistant to vastly all type of pathogens, often antagonize each other, and thus, enhanced resistance against biotrophic pathogens normally leads to increased susceptibility to necrotrophs, and vice versa (Glazebrook, 2005). Solving this trade-off is a major challenge for obtaining broad-spectrum resistance and requires uncoupling the antagonism between these hormonal pathways in crops.

*Pto* DC3000 is the natural causal agent of the bacterial speck disease of tomato. Bacterial spots on tomato fruits have been reported to cause up to 52% loss of fruit weight (Jones et al., 1986), whereas in the field, yield losses due to bacterial speck vary from 75% in plants infected at an early stage of growth to 5% in plants infected later in the season (Yunis et al., 1980). Therefore, it becomes necessary to uncover novel sources of resistance against this pathogen. *Pto* DC3000 uses COR as a virulent factor to induce stomata opening and facilitate entrance into the leaf apoplast. We have recently identified the specific JAZ co-receptor of COR at the stomata in Arabidopsis (Gimenez-Ibanez et al., 2017). A dominant mutation of this stomata-specific AtJAZ2 lacking a C-terminal Jas regulatory domain (*Atjaz2Δjas*) is insensitive to COR and cannot re-open stomata after bacterial infection. This mutation confers resistance to biotrophic *Pto* DC3000 without affecting susceptibility to necrotrophs, due to its specific action at guard cells (Gimenez-Ibanez et al., 2017).

In this study, we demonstrate that similar *Δjas* mutations in stomata-accumulating JAZ proteins can be used as a general strategy to dampen MYC activity is specific tissues and increase resistance to COR-producing bacteria in crops. Thus, as a proof-of-concept, we identified the tomato ortholog of *AtJAZ2* and successfully generated a bacterial speck resistant tomato in the commercial variety Moneymaker by CRISPR/Cas9-mediated *SlJAZ2* editing. *Sljaz2Δjas* plants were significantly more resistant to *Pto* DC3000 when plants where surface inoculated, but equally susceptible by infiltration. This indicates that this SlJAZ2 variant is mainly affecting the stomatal defence layer by counteracting the effect of COR. Consistently, *Sljaz2Δjas* tomato lines were fully impaired in COR-mediated

stomatal reopening. Remarkably, since the *Sljaz2Δjas* mutation only manipulates the JA-dependent defences at the stomata, the JA-SA antagonism is not affected in the mesophyll and, therefore, apoplastic resistance to the necrotrophic pathogen *B. cinerea* remains unaffected. These results suggest that similar to Arabidopsis, SlJAZ2 plays a major role in regulating stomatal aperture during biotic stresses, and that COR produced by *Pto* DC3000 hijacks SlCOI1-SlJAZ2 co-receptor to promote the entry of the bacteria to the internal tissues of tomato leaf. Moreover, these results prove that is possible to uncouple SA-JA antagonism spatially to design novel strategies for protection against COR-producing *P. syringae* strains in crops, without affecting resistance to necrotrophs.

Alteration of the regulation of plant stomatal aperture can lead to deleterious effects. A number of environment factors, including $CO_2$ level, light, water and other abiotic stresses also regulate stomatal dynamics. In all these cases, ABA functions as a chemical messenger that induces stomata closure (Lim et al., 2015; Vishwakarma et al., 2017). However, several lines of evidence suggest that *Sljaz2Δjas* tomato lines are not affected in these ABA-mediated physiological processes. Firstly, in Arabidopsis, gain-of-function mutations in JAZ2 prevent stomatal reopening by COR by inhibiting SA-dependent stomatal closure triggered upon specific microbial perception without affecting ABA signalling at the stomata (Gimenez-Ibanez et al., 2017). Secondly, the rate of stomatal aperture in normal light conditions was not affected in *Sljaz2Δjas* tomato mutants. Thirdly, neither water transpiration rate or leaf temperature was affected in *Sljaz2Δjas* compared to WT. Finally, *Sljaz2Δjas* plants displayed a complete phenotypically normal development compared to WT tomatoes (Supplemental Figure 11). Taken together, these results suggest that the *Sljaz2Δjas* mutation impact on the regulation of stomatal aperture exclusively during biotic conditions, when SA is produced to execute resistance against biotrophic pathogens trying to invade the plant.

Current methods to control bacterial speck disease of tomato are based on removal of plant debris and weeds, crop rotation, and the use of non-infected seeds and transplants. Chemical sprays based on copper are also commonly used, but these may not be effective in environmental conditions favourable for infection (Somodi et al., 1996). Moreover, copper can also kill plant cells if absorbed in sufficient quantities and can produce problematic toxicity in soil. In contrast, tomato resistant varieties offer the most effective means of management. *P. syringae* strains vary in their ability to establish and maintain epiphytic populations on the surface of the leave before infection of internal plant tissues. In this sense, it is becoming clear that transition from epiphytic to endophytic lifestyles is a critical process to establish a successful infection cycle. This transitional process is enhanced by the production of COR. In the case of *Sljaz2Δjas,* these plants would impede the entry on the bacteria, elongating its epiphytic phase where *P. syringae* encounters a harsh environment with limited nutrients. This elongated epiphytic phase on *Sljaz2Δjas* tomatoes should reduce survival of the bacteria further enhancing resistance.

Current resistant varieties are based on the introduction of specific disease resistant genes that recognized pathogenic molecules intracellularly. However, pathogens frequently adapt to and

overcome genetic resistance especially when it is determined by major resistant genes (Brown, 2015). The ability of *Sljaz2Δjas* tomato plants to interfere with the penetration of the pathogen represents a new strategy for providing resistance that may be achieved by a low energetic cost for the plant and in a clean way for the environment. Ultimately, a hierarchical design containing multiple layers of resistance in a crop may be the most feasible way to achieve durable resistant in the field (Fuchs, 2017; Pilet-Nayel et al., 2017).

Recent results demonstrate that novel techniques for genome editing could be successfully applied in crops to introduce directed resistance. For example, CRISPR/Cas has been recently used to generate powdery mildew resistant tomatoes (Nekrasov et al., 2017) and engineer resistance to geminiviruses in tobacco (Ali et al., 2015). Public policies are forcing researchers to develop transgene-free improved crops. In this context DNA editing technologies (also called New Breeding Techniques) have emerged as a novel strategy to overcome this challenge. The status of genetically edited crop varieties is still debated by regulatory authorities, for example countries such as US consider transgene-free genetically edited crops as non-GMO. We hope that plant varieties such as the one presented here could be adopted worldwide to enhance plant productivity and resistance against pests. These superior varieties have the potential to fight against agricultural losses in the field due to pests, reducing the chemical inputs towards a more sustainable agriculture for the environment.

Altogether, we demonstrate the feasibility to create bacterial speck resistant tomatoes through CRISPR/Cas9-mediated editing of *SlJAZ2*. Moreover, we also define a novel strategy to overcome the penetration of COR-producing *P. syringae* strains through the stomata by spatially uncoupling SA-JA antagonism.

# CONCLUSIONS

-MYC proteins act as photomorphogenic TFs that regulate phytochrome responses by regulating PIFs targets and activating *HY5* expression

-SlJAZ2 controls stomata dynamics in response to COR in tomato

-SlJAZ2Δjaz tomato plants edited by CRISPR/Cas9 are more resistant to the pathogenic bacteria *Pseudomonas syringae* DC3000, maintaining also resistance to necrotrophs.

-Las proteínas MYC actúan como factores de transcripción fotomorfogénicos que regulan las respuestas de fitocromos a través de la regulación de genes diana de las PIFs y activando la expresión de *HY5*.

-SlJAZ2 controla el movimiento estomático en respuesta a coronatina en tomate.

-Las plantas de tomate SlJAZ2Δjas editadas mediante la técnica CRISPR/Cas9 son más resistentes a la bacteria *Pseudomonas syringae* DC3000 y mantienen inalterada la resistencia a patógenos necrotrofos.

# REFERENCES

**Abe, H., Urao, T., Ito, T., Seki, M., Shinozaki, K., and Yamaguchi-Shinozaki, K.** (2003). Arabidopsis AtMYC2 (bHLH) and AtMYB2 (MYB) Function as Transcriptional Activators in Abscisic Acid Signaling. Plant Cell **15**: 63–78.

**Ali, Z., Abulfaraj, A., Idris, A., Ali, S., Tashkandi, M., and Mahfouz, M.M.** (2015). CRISPR/Cas9-mediated viral interference in plants. Genome Biol. **16**: 238.

**Von Arnim, A.G. and Deng, X.-W.** (1994). Light inactivation of Arabidopsis Photomorphogenic Repressor COP1 Involves a Cell-Specific Regulation of Its Nucleocytoplasmic Partitioning. Cell **79**: 1035–1045.

**Ballaré, C.L.** (2014). Light Regulation of Plant Defense. Annu. Rev. Plant Biol. **65**: 335–363.

**Ballaré, C.L. and Pierik, R.** (2017). The shade-avoidance syndrome: multiple signals and ecological consequences. Plant. Cell Environ. **40**: 2530–2543.

**Ballesteros, M.L.** (2001). LAF1, a MYB transcription activator for phytochrome A signaling. Genes Dev. **15**: 2613–2625.

**Balmuth, A. and Rathjen, J.P.** (2007). Genetic and molecular requirements for function of the Pto/Prf effector recognition complex in tomato and Nicotiana benthamiana. Plant J. **51**: 978–990.

**Belhaj, K., Chaparro-Garcia, A., Kamoun, S., Patron, N.J., and Nekrasov, V.** (2015). Editing plant genomes with CRISPR/Cas9. Curr. Opin. Biotechnol. **32**: 76–84.

**Bender, C.L., Stone, H.E., Sims, J.J., and Cooksey, D.A.** (1987). Reduced pathogen fitness of Pseudomonas syringae pv. tomato Tn5 mutants defective in coronatine production. Physiol. Mol. Plant Pathol. **30**: 273–283.

**Blancard, D.** (2012). Tomato Diseases (Elsevier).

**Boter, M., Ruíz-Rivero, O., Abdeen, A., and Prat, S.** (2004). Conserved MYC transcription factors play a key role in jasmonate signaling both in tomato and Arabidopsis. Genes Dev. **18**: 1577–91.

**Brodribb, T.J. and McAdam, S.A.M.** (2017). Evolution of the Stomatal Regulation of Plant Water Content. Plant Physiol. **174**: 639–649.

**Brooks, C., Nekrasov, V., Lippman, Z.B., and Van Eck, J.** (2014). Efficient Gene Editing in Tomato in the First Generation Using the Clustered Regularly Interspaced Short Palindromic Repeats/CRISPR-Associated9 System. PLANT Physiol. **166**: 1292–1297.

**Brooks, D.M., Bender, C.L., and Kunkel, B.N.** (2005). The Pseudomonas syringae phytotoxin coronatine promotes virulence by overcoming salicylic acid-dependent defences in Arabidopsis thaliana. Mol. Plant Pathol. **6**: 629–639.

**Brown, J.K.M.** (2015). Durable Resistance of Crops to Disease: A Darwinian Perspective. Annu. Rev. Phytopathol. **53**: 513–539.

**Campos, M.L., Yoshida, Y., Major, I.T., de Oliveira Ferreira, D., Weraduwage, S.M., Froehlich, J.E., Johnson, B.F., Kramer, D.M., Jander, G., Sharkey, T.D., and Howe, G.A.** (2016). Rewiring of jasmonate and phytochrome B signalling uncouples plant growth-defense tradeoffs. Nat. Commun. **7**: 12570.

**Casal, J.J.** (2013). Photoreceptor Signaling Networks in Plant Responses to Shade. Annu. Rev. Plant Biol. **64**: 403–427.

**Chico, J.-M., Fernandez-Barbero, G., Chini, A., Fernandez-Calvo, P., Diez-Diaz, M., and Solano, R.** (2014). Repression of Jasmonate-Dependent Defenses by Shade Involves Differential Regulation of Protein Stability of MYC Transcription Factors and Their JAZ Repressors in Arabidopsis. Plant Cell **26**: 1967–1980.

**Chinchilla, D., Zipfel, C., Robatzek, S., Kemmerling, B., Nürnberger, T., Jones, J.D.G., Felix, G., and Boller, T.** (2007). A flagellin-induced complex of the receptor FLS2 and BAK1 initiates plant defence. Nature **448**: 497–500.

**Chini, A., Ben-Romdhane, W., Hassairi, A., and Aboul-Soud, M.A.M.** (2017). Identification of TIFY/JAZ family genes in Solanum lycopersicum and their regulation in response to abiotic stresses. PLoS One **12**: e0177381.

**Chini, A., Fonseca, S., Fernández, G., Adie, B., Chico, J.M., Lorenzo, O., García-Casado, G., López-Vidriero, I., Lozano, F.M., Ponce, M.R., Micol, J.L., and Solano, R.** (2007). The JAZ family of

repressors is the missing link in jasmonate signalling. Nature **448**: 666–671.

**Chini, A., Gimenez-Ibanez, S., Goossens, A., and Solano, R.** (2016). Redundancy and specificity in jasmonate signalling. Curr. Opin. Plant Biol. **33**: 147–156.

**Deng, X.W., Caspar, T., and Quail, P.H.** (1991). Cop1 : a regulatory locus involved m hght-controlled development and gene expression in Arabidopsis. Genes Dev. **5**: 1172–1182.

**Dharmasiri, N., Dharmasiri, S., Weijers, D., Lechner, E., Yamada, M., Hobbie, L., Ehrismann, J.S., Jürgens, G., and Estelle, M.** (2005). Plant Development Is Regulated by a Family of Auxin Receptor F Box Proteins. Dev. Cell **9**: 109–119.

**Dill, A., Thomas, S.G., Hu, J., Steber, C.M., and Sun, T.-P.** (2004). The Arabidopsis F-box protein SLEEPY1 targets gibberellin signaling repressors for gibberellin-induced degradation. Plant Cell **16**: 1392–405.

**Ding, Y., Li, H., Chen, L.-L., and Xie, K.** (2016). Recent Advances in Genome Editing Using CRISPR/Cas9. Front. Plant Sci. **7**: 1–12.

**Doudna, J.A. and Charpentier, E.** (2014). The new frontier of genome engineering with CRISPR-Cas9. Science (80-. ). **346**.

**Du, M. et al.** (2014). Closely Related NAC Transcription Factors of Tomato Differentially Regulate Stomatal Closure and Reopening during Pathogen Attack. Plant Cell **26**: 3167–3184.

**Duek, P.D. and Fankhauser, C.** (2003). HFR1, a putative bHLH transcription factor, mediates both phytochrome A and cryptochrome signalling. Plant J. **34**: 827–836.

**Feng, J., Liu, T., Qin, B., Zhang, Y., and Liu, X.S.** (2012). Identifying ChIP-seq enrichment using MACS. Nat. Protoc. **7**: 1728–1740.

**Feng, S. et al.** (2008). Coordinated regulation of Arabidopsis thaliana development by light and gibberellins. Nature **451**: 475–479.

**Fernández-Calvo, P. et al.** (2011). The Arabidopsis bHLH Transcription Factors MYC3 and MYC4 Are Targets of JAZ Repressors and Act Additively with MYC2 in the Activation of Jasmonate Responses. Plant Cell **23**: 701–715.

**Fonseca, S., Chico, J.M., and Solano, R.** (2009a). The jasmonate pathway: the ligand, the receptor and the core signalling module. Curr. Opin. Plant Biol. **12**: 539–547.

**Fonseca, S., Chini, A., Hamberg, M., Adie, B., Porzel, A., Kramell, R., Miersch, O., Wasternack, C., and Solano, R.** (2009b). (+)-7-iso-Jasmonoyl-L-isoleucine is the endogenous bioactive jasmonate. Nat. Chem. Biol. **5**: 344–350.

**Franco-Zorrilla, J.M., López-Vidriero, I., Carrasco, J.L., Godoy, M., Vera, P., and Solano, R.** (2014). DNA-binding specificities of plant transcription factors and their potential to define target genes. Proc. Natl. Acad. Sci. **111**: 2367–2372.

**Franklin, K.A., Lee, S.H., Patel, D., Kumar, S.V., Spartz, A.K., Gu, C., Ye, S., Yu, P., Breen, G., Cohen, J.D., Wigge, P.A., and Gray, W.M.** (2011). PHYTOCHROME-INTERACTING FACTOR 4 (PIF4) regulates auxin biosynthesis at high temperature. Proc. Natl. Acad. Sci. **108**: 20231–20235.

**Franklin, K.A. and Quail, P.H.** (2010). Phytochrome functions in Arabidopsis development. J. Exp. Bot. **61**: 11–24.

**Fuchs, M.** (2017). Pyramiding resistance-conferring gene sequences in crops. Curr. Opin. Virol. **26**: 36–42.

**Gangappa, S.N. and Botto, J.F.** (2016). The Multifaceted Roles of HY5 in Plant Growth and Development. Mol. Plant **9**: 1353–1365.

**Gimenez-Ibanez, S., Boter, M., Ortigosa, A., García-Casado, G., Chini, A., Lewsey, M.G., Ecker, J.R., Ntoukakis, V., and Solano, R.** (2017). JAZ2 controls stomata dynamics during bacterial invasion. New Phytol. **213**: 1378–1392.

**Gimenez-Ibanez, S., Hann, D.R., Ntoukakis, V., Petutschnig, E., Lipka, V., and Rathjen, J.P.** (2009). AvrPtoB Targets the LysM Receptor Kinase CERK1 to Promote Bacterial Virulence on Plants. Curr. Biol. **19**: 423–429.

**Gitaitis, R.D., Jones, J.B., Jaworski, C.A., and Phatak, S.C.** (1985). Incidence and development of Pseudomonas syringae pv. syringae on tomato transplants in Georgia. Plant Dis. **69**: 32–35.

**Glazebrook, J.** (2005). Contrasting Mechanisms of Defense Against Biotrophic and Necrotrophic Pathogens. Annu. Rev. Phytopathol. **43**: 205–227.

**Godoy, M., Franco-Zorrilla, J.M., Pérez-Pérez, J., Oliveros, J.C., Lorenzo, Ó., and Solano, R.** (2011). Improved protein-binding microarrays for the identification of DNA-binding specificities of transcription factors. Plant J. **66**: 700–711.

**Guo, Q., Major, I.T., and Howe, G.A.** (2018). Resolution of growth–defense conflict: mechanistic insights from jasmonate signaling. Curr. Opin. Plant Biol. **44**: 72–81.

**Herms, D.A. and Mattson, W.J.** (1992). The Dilemma of Plants: To Grow or Defend. Source Q. Rev. Biol. **67**: 283–335.

**Hisamatsu, T., King, R.W., Helliwell, C. a, and Koshioka, M.** (2005). The involvement of gibberellin 20-oxidase genes in phytochrome-regulated petiole elongation of Arabidopsis. Plant Physiol. **138**: 1106–1116.

**Hong, F., Breitling, R., McEntee, C.W., Wittner, B.S., Nemhauser, J.L., and Chory, J.** (2006). RankProd: A bioconductor package for detecting differentially expressed genes in meta-analysis. Bioinformatics **22**: 2825–2827.

**Hornitschek, P., Kohnen, M. V., Lorrain, S., Rougemont, J., Ljung, K., López-Vidriero, I., Franco-Zorrilla, J.M., Solano, R., Trevisan, M., Pradervand, S., Xenarios, I., and Fankhauser, C.** (2012). Phytochrome interacting factors 4 and 5 control seedling growth in changing light conditions by directly controlling auxin signaling. Plant J. **71**: 699–711.

**Hou, X., Lee, L.Y.C., Xia, K., Yan, Y., and Yu, H.** (2010). DELLAs Modulate Jasmonate Signaling via Competitive Binding to JAZs. Dev. Cell **19**: 884–894.

**Huot, B., Yao, J., Montgomery, B.L., and He, S.Y.** (2014). Growth–Defense Tradeoffs in Plants: A Balancing Act to Optimize Fitness. Mol. Plant **7**: 1267–1287.

**Ishiga, Y., Ishiga, T., Uppalapati, S.R., and Mysore, K.S.** (2013). Jasmonate ZIM-Domain (JAZ) Protein Regulates Host and Nonhost Pathogen-Induced Cell Death in Tomato and Nicotiana benthamiana. PLoS One **8**.

**Jones, J. B., Jones, J. P., Stall, R. E., and Zitter, T.A.** (1991). Compendium of Tomato Diseases. Am. Phytopathol. Soc.

**Jones, J.B., Pohronezny, K.L., Stall, R.E., and Jones, J.P.** (1986). Survival of Xanthomonas campestris pv. vesicatoria in Florida on tomato crop residue, weeds, seeds, and volunteer tomato plants. Phytopathology.

**Katsir, L., Schilmiller, A.L., Staswick, P.E., He, S.Y., and Howe, G.A.** (2008). COI1 is a critical component of a receptor for jasmonate and the bacterial virulence factor coronatine. Proc. Natl. Acad. Sci. **105**: 7100–7105.

**Kazan, K. and Manners, J.M.** (2013). MYC2: The Master in Action. Mol. Plant **6**: 686–703.

**Kharchenko, P. V, Tolstorukov, M.Y., and Park, P.J.** (2008). Design and analysis of ChIP-seq experiments for DNA-binding proteins. Nat. Biotechnol. **26**: 1351–1359.

**Kim, T.-H., Böhmer, M., Hu, H., Nishimura, N., and Schroeder, J.I.** (2010). Guard Cell Signal Transduction Network: Advances in Understanding Abscisic Acid, CO 2 , and Ca 2+ Signaling. Annu. Rev. Plant Biol. **61**: 561–591.

**Kliebenstein, D.J.** (2016). False idolatry of the mythical growth versus immunity tradeoff in molecular systems plant pathology. Physiol. Mol. Plant Pathol. **95**: 55–59.

**Landt, S.G. et al.** (2012). ChIP-seq guidelines and practices of the ENCODE and modENCODE consortia. Genome Res. **22**: 1813–1831.

**Langmead, B. and Salzberg, S.L.** (2012). Fast gapped-read alignment with Bowtie 2. Nat. Methods **9**: 357–359.

**Laurie-Berry, N., Joardar, V., Street, I.H., and Kunkel, B.N.** (2006). The *Arabidopsis thaliana JASMONATE INSENSITIVE 1* Gene Is Required for Suppression of Salicylic Acid-Dependent Defenses During Infection by *Pseudomonas syringae*. Mol. Plant-Microbe Interact. **19**: 789–800.

**Lavy, M. and Estelle, M.** (2016). Mechanisms of auxin signaling. Development **143**: 3226–3229.

**Lee, S., Cheng, H., King, K.E., Wang, W., He, Y., Hussain, A., Lo, J., Harberd, N.P., and Peng, J.** (2002). Gibberellin regulates Arabidopsis seed germination via RGL2,a GAI/RGA-like gene whose expression is up-regulated following imbibition. Genes Dev.

**Leivar, P. and Quail, P.H.** (2011). PIFs: pivotal components in a cellular signaling hub. Trends Plant Sci. **16**: 19–28.

**Lim, C., Baek, W., Jung, J., Kim, J.-H., and Lee, S.** (2015). Function of ABA in Stomatal Defense against Biotic and Drought Stresses. Int. J. Mol. Sci. **16**: 15251–15270.

**Liu, J., Elmore, J.M., Fuglsang, A.T., Palmgren, M.G., Staskawicz, B.J., and Coaker, G.** (2009). RIN4 functions with plasma membrane H+-ATPases to regulate stomatal apertures during pathogen attack. PLoS Biol. **7**.

**Lorenzo, O., Chico, J.M., Sánchez-Serrano, J.J., and Solano, R.** (2004). JASMONATE-INSENSITIVE1 encodes a MYC transcription factor essential to discriminate between different jasmonate-regulated defense responses in Arabidopsis. Plant Cell **16**: 1938–50.

**Lorrain, S.V., Genoud, T., and Fankhauser, C.** (2006). Let there be light in the nucleus! Curr. Opin. Plant Biol. **9**: 509–514.

**de Lucas, M., Davière, J.-M., Rodríguez-Falcón, M., Pontin, M., Iglesias-Pedraz, J.M., Lorrain, S., Fankhauser, C., Blázquez, M.A., Titarenko, E., and Prat, S.** (2008). A molecular framework for light and gibberellin control of cell elongation. Nature **451**: 480–484.

**Mahfouz, M.M., Piatek, A., and Stewart, C.N.** (2014). Genome engineering via TALENs and CRISPR/Cas9 systems: challenges and perspectives. Plant Biotechnol. J. **12**: 1006–1014.

**Mcginnis, K.M., Thomas, S.G., Soule, J.D., Strader, L.C., Zale, J.M., Sun, T.-P., and Steber, C.M.** (2003). The Arabidopsis SLEEPY1 Gene Encodes a Putative F-Box Subunit of an SCF E3 Ubiquitin Ligase. Plant Cell **15**: 1120–1130.

**Medina-Rivera, A. et al.** (2015). RSAT 2015: Regulatory sequence analysis tools. Nucleic Acids Res. **43**: W50–W56.

**Melotto, M., Mecey, C., Niu, Y., Chung, H.S., Katsir, L., Yao, J., Zeng, W., Thines, B., Staswick, P., Browse, J., Howe, G.A., and He, S.Y.** (2008a). A critical role of two positively charged amino acids in the Jas motif of Arabidopsis JAZ proteins in mediating coronatine- and jasmonoyl isoleucine-dependent interactions with the COI1 F-box protein. Plant J. **55**: 979–988.

**Melotto, M., Underwood, W., and He, S.Y.** (2008b). Role of Stomata in Plant Innate Immunity and Foliar Bacterial Diseases. Annu. Rev. Phytopathol. **46**: 101–122.

**Melotto, M., Underwood, W., Koczan, J., Nomura, K., and He, S.Y.** (2006). Plant Stomata Function in Innate Immunity against Bacterial Invasion. Cell **126**: 969–980.

**Melotto, M., Zhang, L., Oblessuc, P.R., and He, S.Y.** (2017). Stomatal Defense a Decade Later. Plant Physiol. **174**: 561–571.

**Mojica, F.J.M., Díez-Villaseñor, C., Soria, E., and Juez, G.** (2000). Biological significance of a family of regularly spaced repeats in the genomes of Archaea, Bacteria and mitochondria. Mol. Microbiol. **36**: 244–246.

**Monte, I., Hamberg, M., Chini, A., Gimenez-Ibanez, S., García-Casado, G., Porzel, A., Pazos, F., Boter, M., and Solano, R.** (2014). Rational design of a ligand-based antagonist of jasmonate perception. Nat. Chem. Biol. **10**: 671–676.

**Moreno, J.E., Tao, Y., Chory, J., and Ballare, C.L.** (2009). Ecological modulation of plant defense via phytochrome control of jasmonate sensitivity. Proc. Natl. Acad. Sci. **106**: 4935–4940.

**Nekrasov, V., Wang, C., Win, J., Lanz, C., Weigel, D., and Kamoun, S.** (2017). Rapid generation of a transgene-free powdery mildew resistant tomato by genome deletion. Sci. Rep. **7**.

**O'Malley, R.C., Huang, S.C., Song, L., Lewsey, M.G., Bartlett, A., Nery, J.R., Galli, M., Gallavotti, A., and Ecker, J.R.** (2016). Cistrome and Epicistrome Features Shape the Regulatory DNA Landscape. Cell **165**: 1280–1292.

**Oliveros, J.C., Franch, M., Tabas-Madrid, D., San-León, D., Montoliu, L., Cubas, P., and Pazos, F.** (2016). Breaking-Cas—interactive design of guide RNAs for CRISPR-Cas experiments for ENSEMBL

genomes. Nucleic Acids Res. **44**: W267–W271.

**Pauwels, L. et al.** (2010). NINJA connects the co-repressor TOPLESS to jasmonate signalling. Nature **464**: 788–791.

**Pfeiffer, A., Shi, H., Tepperman, J.M., Zhang, Y., and Quail, P.H.** (2014). Combinatorial complexity in a transcriptionally centered signaling hub in arabidopsis. Mol. Plant **7**: 1598–1618.

**Pilet-Nayel, M.-L., Moury, B., Caffier, V., Montarry, J., Kerlan, M.-C., Fournet, S., Durel, C.-E., and Delourme, R.** (2017). Quantitative Resistance to Plant Pathogens in Pyramiding Strategies for Durable Crop Protection. Front. Plant Sci. **8**.

**Qi, T., Huang, H., Song, S., and Xie, D.** (2015). Regulation of Jasmonate-Mediated Stamen Development and Seed Production by a bHLH-MYB Complex in Arabidopsis. Plant Cell **27**: 1620–1633.

**Rademacher, W.** (2000). GROWTH RETARDANTS: Effects on Gibberellin Biosynthesis and Other Metabolic Pathways. Annu. Rev. Plant Physiol. Plant Mol. Biol. **51**: 501–531.

**Ritchie, M.E., Silver, J., Oshlack, A., Holmes, M., Diyagama, D., Holloway, A., and Smyth, G.K.** (2007). A comparison of background correction methods for two-colour microarrays. Bioinformatics **23**: 2700–2707.

**Robert-Seilaniantz, A., Grant, M., and Jones, J.D.G.** (2011). Hormone Crosstalk in Plant Disease and Defense: More Than Just JASMONATE-SALICYLATE Antagonism. Annu. Rev. Phytopathol. **49**: 317–343.

**Schneider, R.W.** (1977). Bacterial Speck of Tomato: Sources of Inoculum and Establishment of a Resident Population. Phytopathology **67**: 388–394.

**Schweizer, F., Fernandez-Calvo, P., Zander, M., Diez-Diaz, M., Fonseca, S., Glauser, G., Lewsey, M.G., Ecker, J.R., Solano, R., and Reymond, P.** (2013). Arabidopsis Basic Helix-Loop-Helix Transcription Factors MYC2, MYC3, and MYC4 Regulate Glucosinolate Biosynthesis, Insect Performance, and Feeding Behavior. Plant Cell **25**: 3117–3132.

**Sheard, L.B. et al.** (2010). Jasmonate perception by inositol-phosphate-potentiated COI1–JAZ co-receptor. Nature **468**: 400–405.

**Shinomura, T., Nagatani, a., Chory, J., and Furuya, M.** (1994). The Induction of Seed Germination in Arabidopsis thaliana Is Regulated Principally by Phytochrome B and Secondarily by Phytochrome A. Plant Physiol. **104**: 363–371.

**Somodi, G.C., Jones, J.B., Scott, J.W., Wang, J.F., and Stall, R.E.** (1996). Relationship between the hypersensitive reaction and field resistance to tomato race 1 of Xanthomonas campestris pv. vesicatoria. Plant Dis.

**Song, S., Huang, H., Gao, H., Wang, J., Wu, D., Liu, X., Yang, S., Zhai, Q., Li, C., Qi, T., and Xie, D.** (2014). Interaction between MYC2 and ETHYLENE INSENSITIVE3 Modulates Antagonism between Jasmonate and Ethylene Signaling in Arabidopsis. Plant Cell **26**: 263–279.

**Soukas, A., Cohen, P., Socci, N.D., and Friedman, J.M.** (2000). Leptin-specific patterns of gene expression in white adipose tissue. Genes Dev. **14**: 963–80.

**Staswick, P., Rowe, M., Spalding, E.P., and Splitt, B.L.** (2017). Jasmonoyl-L-Tryptophan Disrupts IAA Activity through the AUX1 Auxin Permease. Front. Plant Sci. **8**.

**Staswick, P.E.** (2009). The Tryptophan Conjugates of Jasmonic and Indole-3-Acetic Acids Are Endogenous Auxin Inhibitors. PLANT Physiol. **150**: 1310–1321.

**Sun, J.-Q., Jiang, H.-L., and Li, C.-Y.** (2011). Systemin/Jasmonate-Mediated Systemic Defense Signaling in Tomato. Mol. Plant **4**: 607–615.

**Thines, B., Katsir, L., Melotto, M., Niu, Y., Mandaokar, A., Liu, G., Nomura, K., He, S.Y., Howe, G.A., and Browse, J.** (2007). JAZ repressor proteins are targets of the SCFCOI1 complex during jasmonate signalling. Nature **448**: 661–665.

**Vishwakarma, K., Upadhyay, N., Kumar, N., Yadav, G., Singh, J., Mishra, R.K., Kumar, V., Verma, R., Upadhyay, R.G., Pandey, M., and Sharma, S.** (2017). Abscisic Acid Signaling and Abiotic Stress Tolerance in Plants: A Review on Current Knowledge and Future Prospects. Front. Plant Sci. **08**.

**de Vries, J., Evers, J.B., and Poelman, E.H.** (2017). Dynamic Plant–Plant–Herbivore Interactions Govern

Plant Growth–Defence Integration. Trends Plant Sci. **22**: 329–337.

**Wasternack, C. and Hause, B.** (2013). Jasmonates: biosynthesis, perception, signal transduction and action in plant stress response, growth and development. An update to the 2007 review in Annals of Botany. Ann. Bot. **111**: 1021–1058.

**de Wit, M., Galvão, V.C., and Fankhauser, C.** (2016). Light-Mediated Hormonal Regulation of Plant Growth and Development. Annu. Rev. Plant Biol. **67**: 513–537.

**Wittmann, J., Brancato, C., Berendzen, K.W., and Dreiseikelmann, B.** (2016). Development of a tomato plant resistant to Clavibacter michiganensis using the endolysin gene of bacteriophage CMP1 as a transgene. Plant Pathol. **65**: 496–502.

**Xie, D.X., Feys, B.F., James, S., Nieto-Rostro, M., and Turner, J.G.** (1998). COI1: an Arabidopsis gene required for jasmonate-regulated defense and fertility. Science **280**: 1091–4.

**Yadav, V., Mallappa, C., Gangappa, S.N., Bhatia, S., and Chattopadhyay, S.** (2005). A basic helix-loop-helix transcription factor in Arabidopsis, MYC2, acts as a repressor of blue light-mediated photomorphogenic growth. Plant Cell.

**Yan, Y., Stolz, S., Chetelat, A., Reymond, P., Pagni, M., Dubugnon, L., and Farmer, E.E.** (2007). A Downstream Mediator in the Growth Repression Limb of the Jasmonate Pathway. PLANT CELL ONLINE **19**: 2470–2483.

**Yang, D.-L. et al.** (2012). Plant hormone jasmonate prioritizes defense over growth by interfering with gibberellin signaling cascade. Proc. Natl. Acad. Sci. U. S. A. **109**: E1192-200.

**Yunis, H., Bashan, Y., Okon, Y., Henis, Y., and others** (1980). Weather dependence, yield losses and control of bacterial speck of tomato caused by Pseudomonas tomato. Plant Dis.

**Zeng, W. and He, S.Y.** (2010). A Prominent Role of the Flagellin Receptor FLAGELLIN-SENSING2 in Mediating Stomatal Response to Pseudomonas syringae pv tomato DC3000 in Arabidopsis. PLANT Physiol. **153**: 1188–1198.

**Zhang, F. et al.** (2015). Structural basis of JAZ repression of MYC transcription factors in jasmonate signalling. Nature **525**: 269–273.

**Zhang, W., He, S.Y., and Assmann, S.M.** (2008a). The plant innate immunity response in stomatal guard cells invokes G-protein-dependent ion channel regulation. Plant J. **56**: 984–996.

**Zhang, Y., Liu, T., Meyer, C.A., Eeckhoute, J., Johnson, D.S., Bernstein, B.E., Nussbaum, C., Myers, R.M., Brown, M., Li, W., and Liu, X.S.** (2008b). Model-based Analysis of ChIP-Seq (MACS). Genome Biol. **9**: R137.

**Zhang, Y., Mayba, O., Pfeiffer, A., Shi, H., Tepperman, J.M., Speed, T.P., and Quail, P.H.** (2013). A Quartet of PIF bHLH Factors Provides a Transcriptionally Centered Signaling Hub That Regulates Seedling Morphogenesis through Differential Expression-Patterning of Shared Target Genes in Arabidopsis. PLoS Genet. **9**: 11–13.

**Zhang, Y. and Turner, J.G.** (2008). Wound-Induced Endogenous Jasmonates Stunt Plant Growth by Inhibiting Mitosis. PLoS One **3**: e3699.

**Zheng, X.Y., Spivey, N.W., Zeng, W., Liu, P.P., Fu, Z.Q., Klessig, D.F., He, S.Y., and Dong, X.** (2012). Coronatine promotes pseudomonas syringae virulence in plants by activating a signaling cascade that inhibits salicylic acid accumulation. Cell Host Microbe **11**: 587–596.

**Zheng, Y., Cui, X., Su, L., Fang, S., Chu, J., Gong, Q., Yang, J., and Zhu, Z.** (2017). Jasmonate inhibits COP1 activity to suppress hypocotyl elongation and promote cotyledon opening in etiolated Arabidopsis seedlings. Plant J. **90**: 1144–1155.

**Zhu, L.J., Gazin, C., Lawson, N.D., Pagès, H., Lin, S.M., Lapointe, D.S., and Green, M.R.** (2010). ChIPpeakAnno: a Bioconductor package to annotate ChIP-seq and ChIP-chip data. BMC Bioinformatics **11**: 237.

**Zipfel, C., Robatzek, S., Navarro, L., Oakeley, E.J., Jones, J.D.G., Felix, G., and Boller, T.** (2004). Bacterial disease resistance in Arabidopsis through flagellin perception. Nature **428**: 764–767.

# SUPLEMENTARY DATA

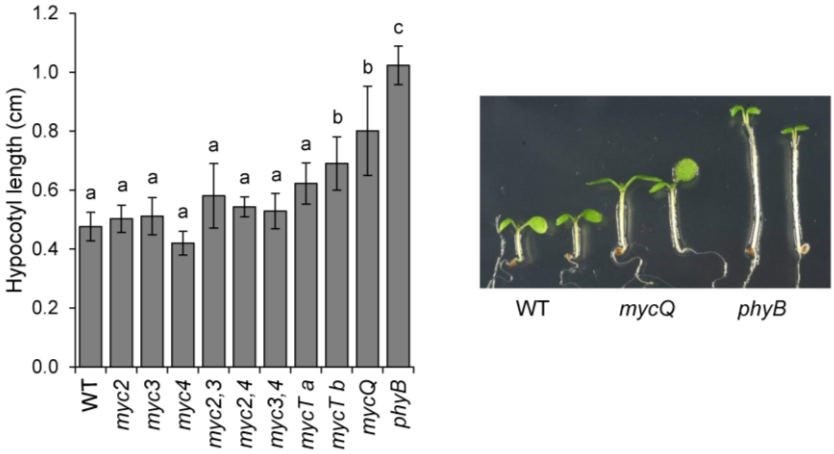


**Supplemental Figure 1.** *myc* multiple mutants show *phyB*-related phenotypes. Hypocotyl length analysis in low white light (LWL) conditions of WT, *phyB* and different single and multiple *myc* mutants. a and b in *mycT* represent two independent triple mutant lines. Error bars represent SD. Letters above bars represent statistically distinct groups.

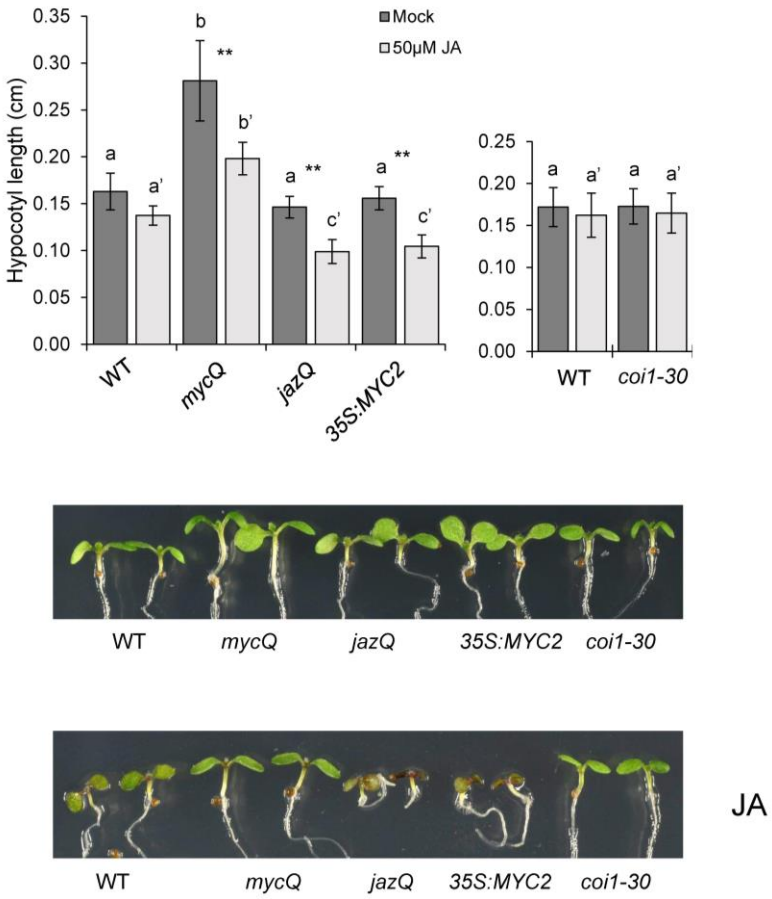


**Supplemental Figure 2.** Photomorphogenic activity of MYC TFs is partially independent of JA and the JA-pathway. Hypocotyl length of WT, *mycQ*, *jazQ*, 35:MYC2 and *coi1-30* in white light conditions. Error bars represent SD. Letters above bars represent statistically distinct groups among mock samples or among JA treated samples. Asterisks represent significant differences between the two conditions of a genotype.

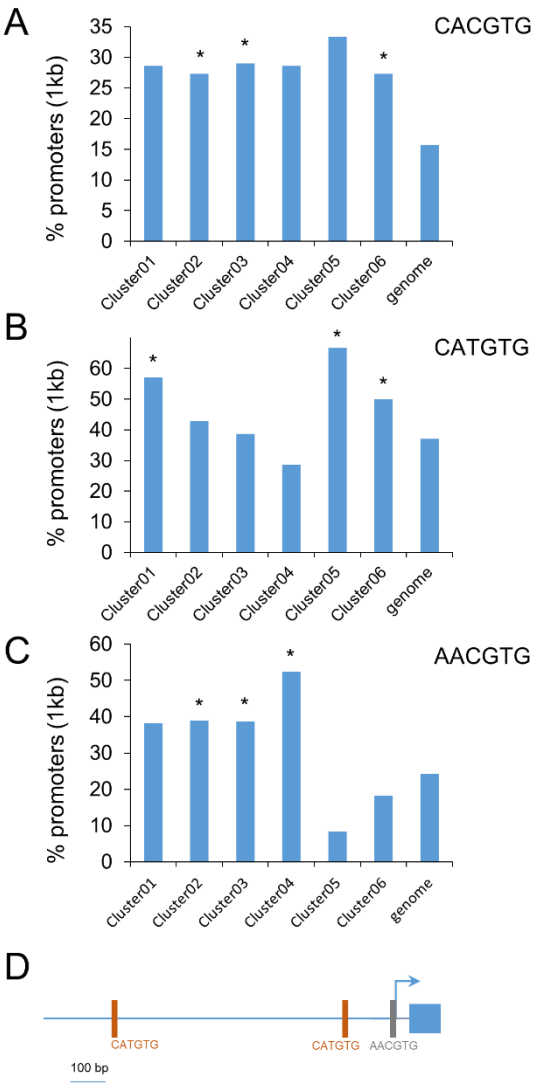


**Supplemental Figure 3. (A)** Percentage of promoters (1 kb upstream the transcription start site, TSS) containing the canonical G-box (CACGTG) in each of the gene clusters obtained in Figure 6. Asterisks denote significant over-representation of the G-box element in the promoters of the clusters indicated relative to the proportion of the G-box in the entire Arabidopsis promoter set (p value < 0.05, hypergeometric test). **(B)** and (**C)**, same as in (A) but referred to the G-related boxes CATGTG (B) and AACGTG (C). **(D)** Graphical representation of G-related boxes in the HY5 promoter region. The enriched MYC2/MYC3 bound region corresponds to the CATGTG element (also called PIF Binding Element, PBE) closest to the TSS (-138 bp upstream).

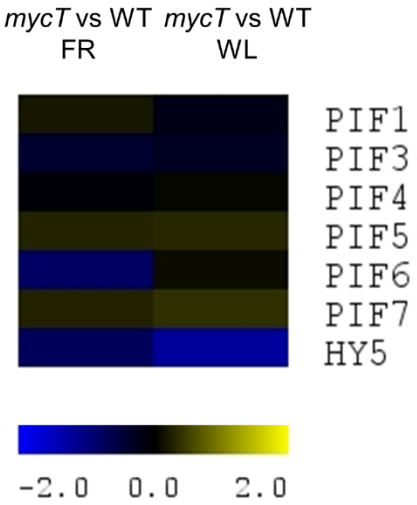


**Supplemental Figure 4.** Expression of PIF genes is not affected in *mycT* mutant. Heat map representation of the log2 ratio (*mycT*/wt) values for the *PIF* genes indicated and *HY5* obtained in our gene expression profiles of *mycT* in Far Red (FR) and White Light conditions (WL).

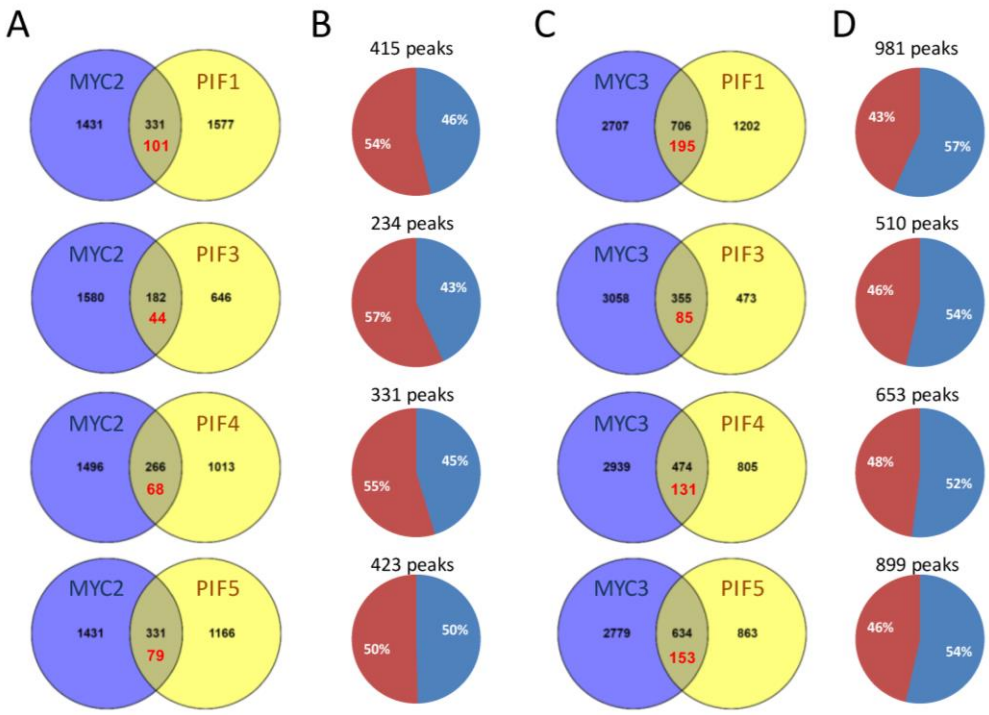


**Supplemental Figure 5.** Large overlapping of MYCs and PIFs target gene sets.

**(A)** and (**C),** Venn diagrams showing overlapping of the target genes of MYC2 (A) or MYC3 (C) and PIFs (PIF1, PIF3, PIF4 or PIF5). The expected number of common targets by chance is indicated in red. In all cases, differences between observed and expected values were significant (P value < 1.0 E-100, Chi-square).

**(B)** and (**D),** percentage of coincident (blue) and non-coincident (red) peaks bound by MYCs and PIFs among shared target genes.


**Supplemental Figure 6**. Examples of PIFs and MYCs targets with shared bound sites. Genome Browser captures of the genes from clusters 1 to 6 not shown in Figure 7 (the number of the cluster indicated in brackets). The panels represent PIFs and MYCs bound fragments determined by ChIP-Seq. High confidence PIF- and MYC-bound intervals are represented as colored arrows in each track. The position of PIF/MYC binding sequences G-box (CACGTG) and PBE (CATGTG) is indicated in red. Horizontal bars correspond to 1 kb.

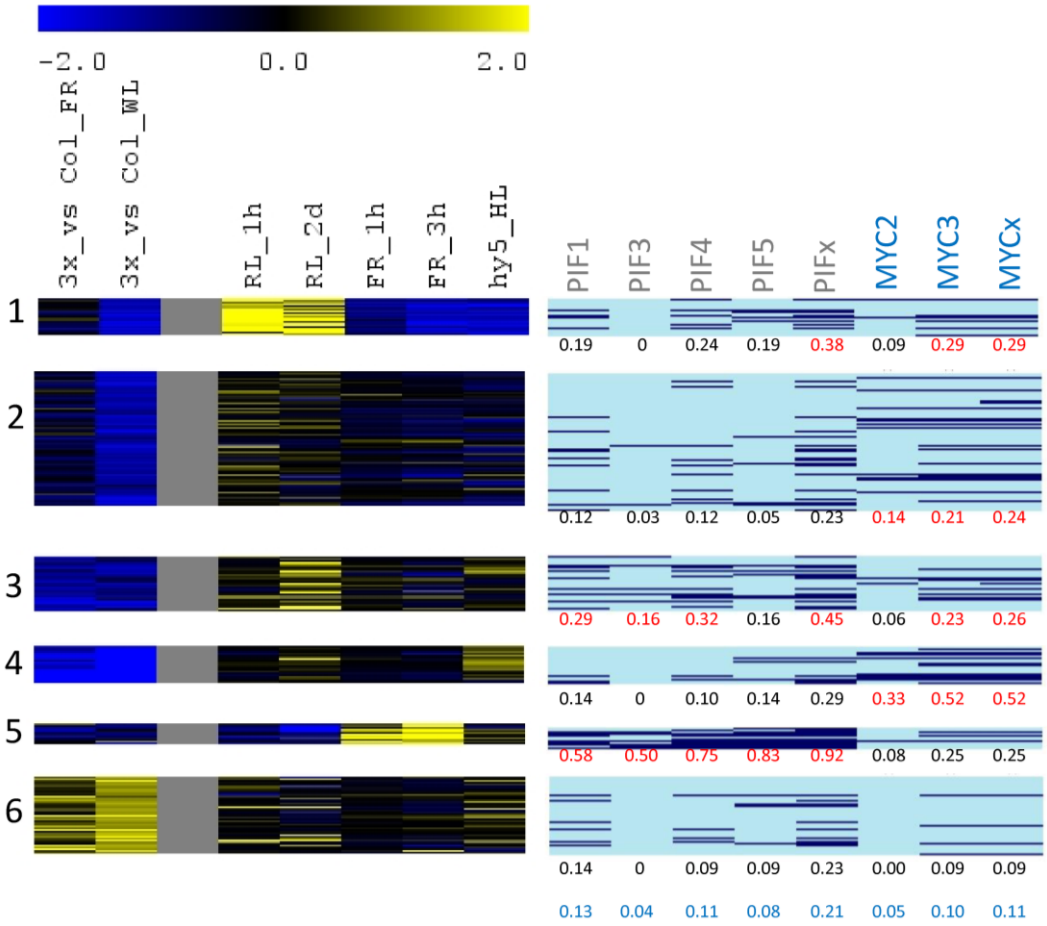


**Supplemental Figure 7.** Over-representation of MYCs and PIFs targets among the genes differentially expressed in *mycT*.

Right, direct target genes of the MYC and PIF TFs determined by ChIP-Seq are represented as dark blue lines over a light blue background. Genes are represented in the same order as in the heat map for clustering analysis (left panel). The proportion of target genes of each TF in each cluster is indicated below each panel, where red numbers denote statistical over-representation over the whole genome proportion (p value < 0.05, hypergeometric test). PIFx and MYCx represent the combination of all (non-redundant) PIF and MYC targets, respectively.

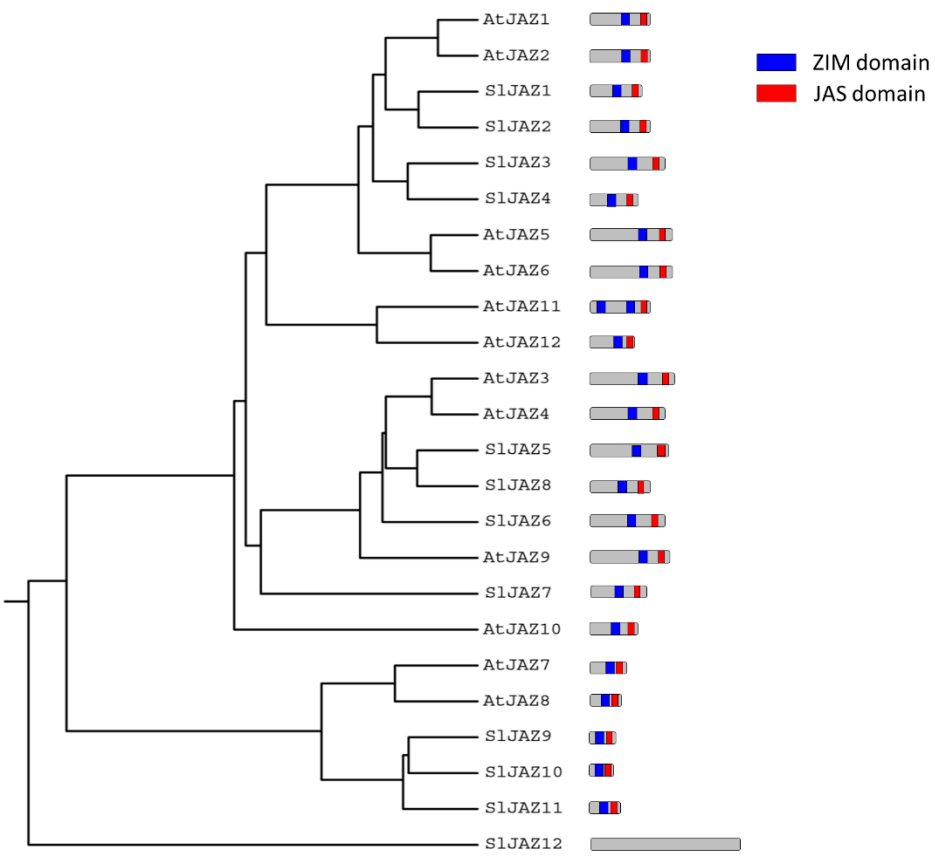


**Supplemental Figure 8:** Phylogenetic tree of all AtJAZs and SlJAZs. The schematic representation indicates length and domains of each JAZ protein.

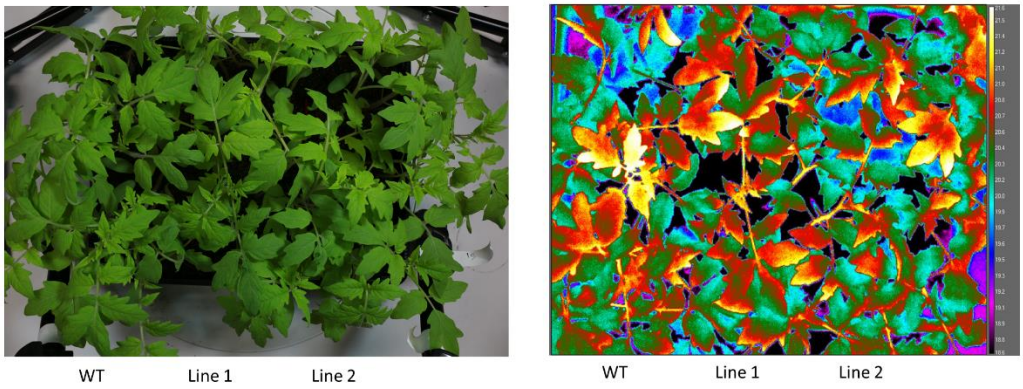


**Supplemental Figure 9:** False color infrared image shows no differences between WT and *Sljaz2Δjas* plants. On the left, image of WT and *Sljaz2Δjas* tomato plants (Line 1 and Line 2), as depicted in the figure, taken with a reflex camera. On the right, the same plants analyzed under an infrared camera to measure leaf temperature.

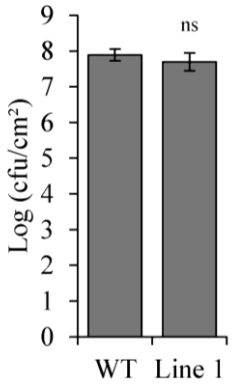


**Supplemental Figure 10. *Sljaz2Δjas* mutant is equally resistant to *Pto* DC3000 COR- when surface inoculated.** Growth of *Pto* DC3000 COR- on WT and *Sljaz2Δjas* (Line 1) tomato plants 7 days after surface inoculation by dipping with bacteria at $10^8$ cfu/ml. Error bars indicate SEM (n=7).


**Supplemental Figure 11:** *Sljaz2Δjaz* plants display a normal phenotype**.**

**Supplemental Table 1:** RT-PCR oligonucleotides used in this study.

| Q-pcr oligonucleotides | Sequence |
|---|---|
| ***SlACTIN* FW** | CAAGTTATTACCATTGGTGCTGAGA |
| ***SlACTIN* RV** | TGCAGCTTCCATACCAATCATG |
| ***SlJAZ1* FW** | GGAAACAATCCTGCTAAACCA |
| ***SlJAZ1* RV** | TCCGAAACTCGGAACCAC |
| ***SlJAZ2* FW** | AAGACAGAATCTTGGAAACCTGA |
| ***SlJAZ2* RV** | AACAATGACTTGTCCACCATAAAA |
| ***SlJAZ3* FW** | AACACCTCCAGATTAAGCCAGAC |
| ***SlJAZ3* RV** | AATTGTGCTTGTGCTGTTGC |
| ***SlJAZ4* FW** | TGGAAAAGCAAATATCAATGATCTAA |
| ***SlJAZ4* RV** | ACAAATCCTTTGTTGCTGAGG |
| **P1** | CAGCTGATCAATCTGGTGTGA |
| **P2** | ATCAGCAACAGAAGGCTGTG |
| **P3** | ATTGGTAAATCAGCAACTGTG |
| **P4** | GTAAATCAGCAACAGCTGTG |

**Supplemental Table 2:** Oligonucleotides used as gRNAs in this study.

| Oligonucleotides used as guide RNA | Sequence |
|---|---|
| **1º gRNA for *SlJAZ2* (A)** | ATTGAAATCAGCAACAGAAGGCTG |
| **1º gRNA for *SlJAZ2* (B)** | AAACCAGCCTTCTGTTGCTGATTT |
| **2º gRNA for *SlJAZ2* (A)** | ATTGCTGATTTACCAATCGCGAGA |
| **2º gRNA for *SlJAZ2* (B)** | AAACTCTCGCGATTGGTAAATCAG |

**Supplemental Table 3.** Enriched Gene Ontology terms (GO Biological Process) in gene clusters shown in Figure 6. GO enrichments were calculated with DAVID Functional Annotation Tool (https://david.ncifcrf.gov/) using default parameters (modified Fisher Exact P-Value and Benjamini multi-test adjustment (Benjamini)).

Cluster 1

| Term | PValue | Benjamini |
|---|---|---|
| GO:0080167~response to karrikin | 4.95E-13 | 3.51E-11 |
| GO:0010224~response to UV-B | 4.92E-09 | 1.75E-07 |
| GO:0009813~flavonoid biosynthetic process | 3.89E-07 | 9.21E-06 |
| GO:0010218~response to far red light | 1.27E-03 | 2.22E-02 |
| GO:0010114~response to red light | 1.77E-03 | 2.48E-02 |
| GO:0071490~cellular response to far red light | 2.16E-03 | 2.53E-02 |
| GO:0071491~cellular response to red light | 2.16E-03 | 2.53E-02 |
| GO:0009733~response to auxin | 3.57E-03 | 3.56E-02 |
| GO:0008152~metabolic process | 4.03E-03 | 3.52E-02 |
| GO:0071492~cellular response to UV-A | 5.39E-03 | 4.18E-02 |
| GO:0052696~flavonoid glucuronidation | 6.43E-03 | 4.48E-02 |
| GO:0071483~cellular response to blue light | 6.47E-03 | 4.10E-02 |
| GO:0010117~photoprotection | 7.54E-03 | 4.38E-02 |
| GO:0046283~anthocyanin-containing compound metabolic process | 7.54E-03 | 4.38E-02 |
| GO:0071486~cellular response to high light intensity | 8.62E-03 | 4.62E-02 |
| GO:0009753~response to jasmonic acid | 1.22E-02 | 6.01E-02 |
| GO:0031540~regulation of anthocyanin biosynthetic process | 1.29E-02 | 5.96E-02 |
| GO:0010380~regulation of chlorophyll biosynthetic process | 1.50E-02 | 6.50E-02 |
| GO:0009698~phenylpropanoid metabolic process | 1.82E-02 | 7.40E-02 |
| GO:0010030~positive regulation of seed germination | 1.93E-02 | 7.40E-02 |
| GO:0009718~anthocyanin-containing compound biosynthetic process | 2.04E-02 | 7.40E-02 |
| GO:0034605~cellular response to heat | 2.78E-02 | 9.51E-02 |
| GO:0009411~response to UV | 2.88E-02 | 9.41E-02 |

Cluster 2

| Term | PValue | Adj. Pvalue |
|---|---|---|
| GO:0080167~response to karrikin | 4.37E-06 | 6.81E-04 |
| GO:0019761~glucosinolate biosynthetic process | 2.37E-04 | 1.83E-02 |
| GO:0052696~flavonoid glucuronidation | 5.42E-04 | 2.78E-02 |
| GO:0010224~response to UV-B | 1.12E-03 | 4.29E-02 |
| GO:0009813~flavonoid biosynthetic process | 1.42E-03 | 4.34E-02 |
| GO:0006979~response to oxidative stress | 2.90E-03 | 7.27E-02 |
| GO:0008152~metabolic process | 3.44E-03 | 7.40E-02 |
| GO:0009699~phenylpropanoid biosynthetic process | 6.12E-03 | 1.13E-01 |
| GO:0055114~oxidation-reduction process | 1.24E-02 | 1.95E-01 |
| GO:0009800~cinnamic acid biosynthetic process | 1.66E-02 | 2.30E-01 |
| GO:0009636~response to toxic substance | 1.78E-02 | 2.25E-01 |
| GO:0008652~cellular amino acid biosynthetic process | 2.25E-02 | 2.56E-01 |
| GO:0006559~L-phenylalanine catabolic process | 2.65E-02 | 2.76E-01 |
| GO:0010439~regulation of glucosinolate biosynthetic process | 2.98E-02 | 2.86E-01 |
| GO:0051555~flavonol biosynthetic process | 2.98E-02 | 2.86E-01 |

Cluster 3

| Term | PValue | Adj. Pvalue |
|---|---|---|
| GO:0009409~response to cold | 1.03E-05 | 6.80E-04 |
| GO:0006970~response to osmotic stress | 2.51E-04 | 8.25E-03 |
| GO:0009414~response to water deprivation | 2.75E-03 | 5.88E-02 |
| GO:0009737~response to abscisic acid | 7.21E-03 | 1.13E-01 |
| GO:0010017~red or far-red light signaling pathway | 2.54E-02 | 2.88E-01 |

Cluster 4

| Term | PValue | Adj. Pvalue |
|---|---|---|
| GO:0019761~glucosinolate biosynthetic process | 4.67E-29 | 2.48E-27 |
| GO:0009625~response to insect | 1.46E-08 | 3.88E-07 |
| GO:0009684~indoleacetic acid biosynthetic process | 7.28E-07 | 1.29E-05 |
| GO:0009098~leucine biosynthetic process | 1.64E-06 | 2.18E-05 |
| GO:0055114~oxidation-reduction process | 4.03E-05 | 4.27E-04 |
| GO:0052544~defense response by callose deposition in cell wall | 1.32E-04 | 1.17E-03 |
| GO:0009682~induced systemic resistance | 1.68E-04 | 1.27E-03 |
| GO:0009082~branched-chain amino acid biosynthetic process | 2.09E-04 | 1.38E-03 |
| GO:0006569~tryptophan catabolic process | 2.16E-03 | 1.27E-02 |
| GO:0033506~glucosinolate biosynthetic process from homomethionine | 3.24E-03 | 1.71E-02 |
| GO:0010120~camalexin biosynthetic process | 1.08E-02 | 5.08E-02 |
| GO:0009611~response to wounding | 1.93E-02 | 8.23E-02 |
| GO:0009718~anthocyanin-containing compound biosynthetic process | 2.04E-02 | 8.04E-02 |
| GO:0006952~defense response | 3.25E-02 | 1.18E-01 |
| GO:0042742~defense response to bacterium | 3.53E-02 | 1.19E-01 |
| GO:0002229~defense response to oomycetes | 3.61E-02 | 1.15E-01 |

Cluster 5

| Term | PValue | Adj. Pvalue |
|---|---|---|
| GO:0009734~auxin-activated signaling pathway | 8.87E-02 | 8.71E-01 |

Cluster 6

| Term | PValue | Adj. Pvalue |
|---|---|---|
| GO:0006952~defense response | 8.14E-04 | 9.08E-02 |
| GO:0006882~cellular zinc ion homeostasis | 8.62E-03 | 3.97E-01 |
| GO:0030026~cellular manganese ion homeostasis | 2.23E-02 | 5.84E-01 |
| GO:0055062~phosphate ion homeostasis | 2.40E-02 | 5.08E-01 |
| GO:0009753~response to jasmonic acid | 2.97E-02 | 5.06E-01 |
| GO:0010025~wax biosynthetic process | 3.91E-02 | 5.40E-01 |
| GO:0050832~defense response to fungus | 4.54E-02 | 5.40E-01 |
| GO:0009908~flower development | 4.75E-02 | 5.09E-01 |